Progress in Oceanography 211 (2023) 102977

Contents lists available at ScienceDirect

Progress in Oceanography

journal homepage: www.elsevier.com/locate/pocean

The marine carbonate system variability in high meltwater season (Spitsbergen Fjords, Svalbard)

Katarzyna Koziorowska-Makuch [a,b,*], Beata Szymczycha [a], Helmuth Thomas [b], Karol Kuliński [a]

[a] Institute of Oceanology Polish Academy of Sciences, Sopot, Poland
[b] Helmholtz-Zentrum Hereon, Institute of Carbon Cycles, Geesthacht, Germany

ARTICLE INFO

Keywords:
Alkalinity
Saturation state of aragonite
pH
pCO_2
Ocean acidification

ABSTRACT

The spatial variability in hydrography (salinity and temperature) and carbonate chemistry (alkalinity - A_T, total inorganic carbon concentration - C_T, pH, CO_2 partial pressure - pCO_2, and the saturation state of aragonite - Ω_{Ar}) in high meltwater season (summer) was investigated in four Spitsbergen fjords - Krossfjorden, Kongsfjorden, Isfjorden, and Hornsund. It was found that the differences in hydrology entail spatial changes in the CO_2 system structure. A_T decline with decreasing salinity was evident, hence it is clear that freshwater input generally has a diluting effect and lowers A_T in the surface waters of the Spitsbergen fjords. Significant surface water A_T variability (1889–2261 μmol kg^{-1}) reveals the complexity of the fjords' systems with multiple freshwater sources having different alkalinity end-member characteristics and identifies the mean A_T freshwater end-member of 595 ± 84 μmol kg^{-1} for the entire region. The effect of A_T fluxes from sediments on the bottom water was rather insignificant, despite high A_T values (2288–2666 μmol kg^{-1}) observed in the pore waters. Low pCO_2 results in surface water (200–295 μatm) points to intensive biological production, which can strongly affect the C_T values, however, is less important for shaping alkalinity. It has also been shown that the freshening of the surface water in the fjords reduces significantly Ω_{Ar} (an increase in freshwater fraction contribution by 1% causes a decrease in Ω_{Ar} by 0.022). Although during the polar day, due to low pCO_2, Ω_{Ar} values are still rather far from 1 (they ranged from 1.4 to 2.5), during polar night, when pCO_2 values are much higher, Ω_{Ar} may drop markedly. This study highlights that the use of salinity to estimate the potential alkalinity can carry a high uncertainty, while good recognition of the surface water A_T variability and its freshwater end-members is key to predict marine CO_2 system changes along with the ongoing freshening of fjords waters due to climate warming.

1. Introduction

Over the last several decades an increase in carbon dioxide concentrations in the atmosphere has been observed, which is mainly caused by anthropogenic activities, such as fossil fuels combustion, cement production, and land-use changes (IPCC, 2019). This results not only in global warming but also leads to the enhanced dissolution of CO_2 in the ocean. It is estimated that the global ocean absorbs about 22% of anthropogenic CO_2 emissions (Le Quere et al., 2018). Since CO_2 dissolved in seawater forms the diprotic carbonic acid, hydrogen ions are released. Although the major fraction of the hydrogen ions is buffered by carbonate ions (buffer reaction), a significant fraction stays in the water column causing decrease in pH (Eq. (1)).

$$CO_{2(g)} \Leftrightarrow CO_{2(aq)} \Leftrightarrow H_2CO_3 \Leftrightarrow H^+ + HCO_3^- \Leftrightarrow 2H^+ + CO_3^{2-} \quad (1)$$

This phenomenon is known in the scientific literature as "ocean acidification" and has been recognized as one of the greatest threats for marine ecosystems, especially for calcifying organisms, which at lower pH may have difficulties in developing exoskeletons (Gazeau et al., 2007). The scale of ocean acidification depends on the buffer capacity of seawater, which can be approximated with total alkalinity. A_T of seawater is defined as an excess of proton acceptors - bases, over proton donors - acids (Dickson, 1981). Together with the three other parameters: pH, pCO_2, C_T, total alkalinity is the elementary parameter describing marine CO_2 system. The open ocean surface A_T is relatively constant, however, in coastal areas the alkalinity is much more variable. This is the result of several processes affecting marine CO_2 system in different, sometimes counteracting ways: freshwater input, calcification, $CaCO_3$ dissolution, photosynthesis, respiration and A_T formation and release from sediments in the course of early diagenesis (e.g.

* Corresponding author at: Institute of Oceanology Polish Academy of Sciences, Powstańców Warszawy 55, 81-712, Sopot, Poland.
E-mail address: kkozio@iopan.pl (K. Koziorowska-Makuch).

https://doi.org/10.1016/j.pocean.2023.102977
Received 22 December 2021; Received in revised form 2 December 2022; Accepted 23 January 2023
Available online 27 January 2023

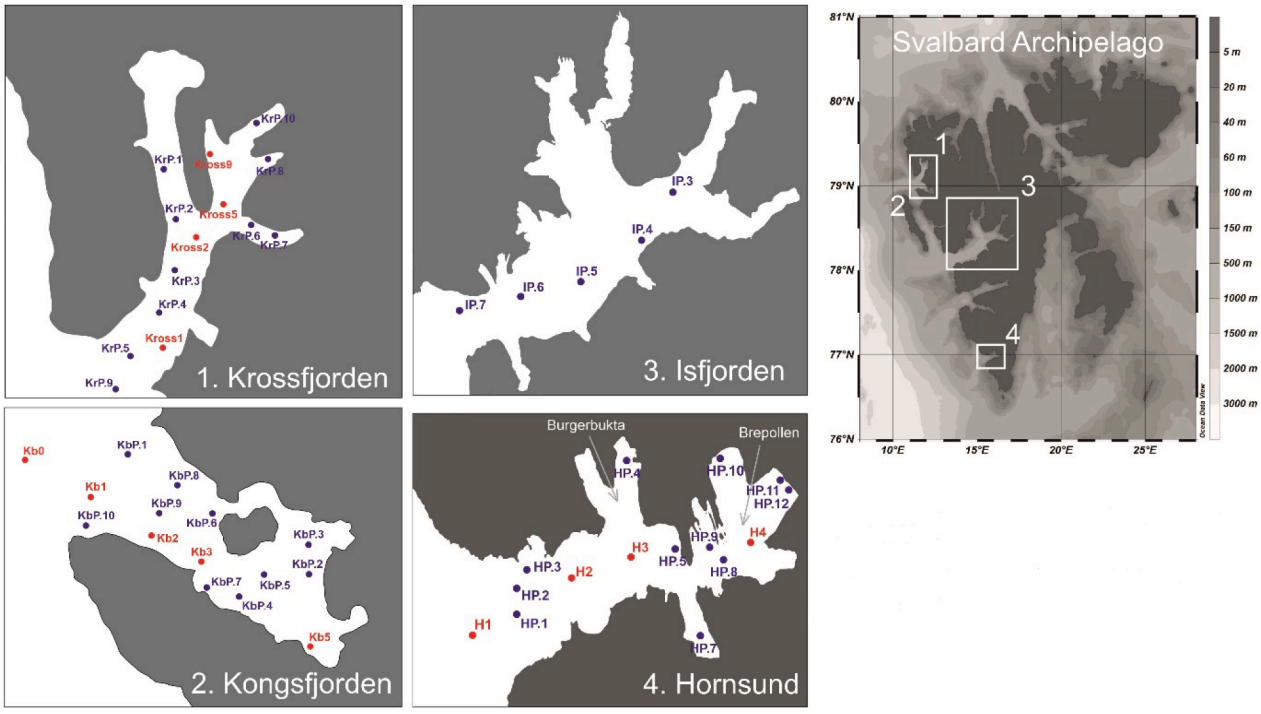

Fig. 1. Location of the sampling stations. Surface water stations are marked in blue, water column profiles and pore water stations are marked in red.

denitrification or pyrite formation; Cai et al., 2010; Krumins et al., 2013; Brenner et al., 2016; Middelburg, 2019). In the Polar Regions, the situation becomes even more complex, as all processes related to formation and transport of the sea ice, melting and calving glaciers can significantly affect the seawater alkalinity but also other parameters of the marine CO_2 system. It is worth mentioning that these regions are believed to be the most exposed to ocean acidification and consequences of climate warming (Meredith et al., 2019). Moreover, they strongly act as a sink for atmospheric CO_2 thus reducing its negative influence on climate. It was estimated that the Arctic Ocean takes up CO_2 on the order of 66 to 199 Tg C y^{-1}, which constitutes about 5–14% of the total sink for the global ocean (Bates and Mathis, 2009). Additionally, in the Arctic coastal regions, the temperature increase leads to several coupled processes that may affect total alkalinity and thus seawater pH (Shadwick et al., 2013). Increased freshwater supply from both direct input of glacial ice and meltwater (calving and ablation), precipitation, river runoff and sea ice melting (Beszczyńska-Moller et al., 1997; Svendsen et al., 2002; Blaszczyk et al., 2013) dilute seawater and lead usually to reduction of the buffering capacity (A_T) of coastal Arctic waters, which induces pH changes. On the other hand, enhanced weathering of silicate and carbonate rocks (e.g. dolomite, limestone, and marble) in the catchment may partially compensate the dilution effect. Cooper et al. (2008) found the average A_T for the six largest Arctic to be ~ 1048 μmol kg^{-1} (for Yukon river, A_T can even exceed 2068 μmol kg^{-1}), however, most of the results are still below the values measured for seawater. Increased freshwater supply together with the release of nutrients and organic matter (OM) pool frozen in permafrost (Schuur et al., 2015) can also affect the functioning and structure of marine ecosystems (Li et al., 2009; Carmack et al., 2016). It was found that freshwater supply can have either positive (e.g. enhanced vertical fluxes of macronutrients) or negative (e.g. high sediment load that limits light penetration into the water column, or strong, near-surface stratification) effect on primary production in the Arctic coastal regions (Gerringa et al., 2012; Meire et al., 2015; Hopwood et al., 2020) and consequently affect the marine CO_2 system variability. Additionally, brine rejection and ikaite precipitation during sea ice formation have the potential to alter the marine CO_2 system structure. The processes are, however, still poorly understood (Rysgaard et al., 2012a; Fransson et al., 2020).

Although, the Arctic fjords have been discussed as one of the "Aquatic Critical Zones (ACZs)" that need intensive and comprehensive investigation in the face of continuing global warming (Bianchi et al., 2020), still relatively little is known about the marine CO_2 system variability in those regions. Moreover, a small amount of data related to this topic is often restricted to individual locations in the fjords, which limits broader interpretation (Fransson et al., 2015b; Fransson et al., 2016; Ericson et al., 2019a; Ericson et al., 2019b). Hence, in this paper, we (1) present spatial variability in hydrography (salinity, temperature) and carbonate chemistry (A_T, C_T, pH, pCO_2, and the saturation state of aragonite - Ω_{Ar}) in high meltwater season (summer) in four Spitsbergen fjords - Krossfjorden, Kongsfjorden, Isfjorden, and Hornsund; (2) compare the results between investigated fjords (e.g. different hydrology and catchment characteristics); (3) define potential sources of alkalinity anomalies in the waters of the studied fjords and (4) investigate the effect of seawater freshening (e.g. glacial drainage water, river water) on the marine CO_2 system structure.

2. Study area

A lot of research define the Spitsbergen fjords (Svalbard) as Arctic regions mostly affected by the climate change, which is mainly due to the progressive increase of the Atlantic water inflow and the so called Atlantification of the area (Promińska et al., 2018; Vihtakari et al., 2018; Holmes et al., 2019). Therefore, four fjords - Krossfjorden, Kongsfjorden, Isfjorden, and Hornsund, located along the west coast of Spitsbergen were selected for this study (Fig. 1). The system formed by Krossfjorden and Kongsfjorden consists of two submarine channels, which converge to a deep glacial basin, the Kongsfjordrenna. The total area of the drainage basins of both fjords is 3074 km^2, of which 67% of the land area in Krossfjorden and 77% in Kongsfjorden is covered by glaciers. These are: in Krossfjorden - Lilliehookbroon and five smaller glaciers along its eastern coast, and in Kongsfjorden - Kronebreen and Kongsvegen at the fjords' head, Conwaybreen and Blomstrandbreen on the northern coast

(Svendsen et al., 2002). Both fjords are largely influenced by the presence of these tidewater glaciers, thus glacial discharge plays the major contribution of fresh water into the fjords (Maclachlan et al., 2011). Both these fjords differ in terms of bedrock geology. Krossfjorden is comprised of Mesoprotozoic basement – marbles, dolomite marble, mica schist and migmatite. In Kongsfjorden, the northern side is also comprised of Mesoproterozoic basement, whereas, towards south sandstones, silicide carbonate, dolomite, limestone, phyllite and quartz-carbonate schist predominate (Streuff, 2013; Husum et al., 2019). Isfjorden is the largest fjord system on the Spitsbergen (3084 km^2) with the second largest drainage basin (40% is covered by glaciers and only nine tidewater glaciers terminate into the fjord system). Although this is the area with the least relative glacier cover on the island (Hagen, 1993), glacial melt is still probably the most important freshwater source (Nilsen et al., 2008). The bedrock geology is mostly dominated by metamorphic and sedimentary rocks in the western area and volcanic and metamorphic rocks in the east and northeast areas (Dallmann et al., 2002). Hornsund is the southernmost, medium-size fjord (311 km^2) with a complex coastline including a large number of bays (the largest – Brepollen) (Beszczyńska-Moller et al., 1997). The entire drainage basin area is 1200 km^2 and around 67% is covered by 14 glaciers which are the main source of freshwater (Blaszczyk et al., 2013). The bedrock in Hornsund mainly represents Mesozoic strata consist of phyllite, shales, sandstones, and is relatively younger compared to the above described fjords (Kim et al., 2020).

3. Materials and methods

3.1. Sampling

Samples were collected from r/v Oceania in summer 2018 in four fjords – Krossfjorden, Kongsfjorden, Isfjorden, and Hornsund (sampling time: 08.08–10.08, 05.08–08.08, 03.08 and 26.07–01.08, respectively). At some stations (Fig. 1, stations marked in blue) sampling was performed only from the surface water layer (0–1 m), while at the other (Fig. 1 stations marked in red) it also included 5 depths from the water column selected based on the salinity profiles, water overlying the sediment, and pore water collected using Rhizon samplers from the upper 5 cm thick sediment layer. The full set of parameters measured within this study included: A_T, C_T, temperature and salinity. All the water samples were collected according to the commonly used techniques, described briefly below.

3.1.1. Salinity and temperature

Temperature (T) and salinity (S) were measured *in situ* using a CTD SeaBird profiler, 911-Plus.

3.1.2. C_T and A_T

Unfiltered water samples were collected in 250-ml glass bottles (avoiding gas exchange), poisoned with 100 μl of the saturated $HgCl_2$ solution, and stored in a dark at 4 °C until analyses. The C_T was measured in a TOC-L analyzer (Shimadzu Corp., Japan). The measurement method is based on sample acidification and detection of the evolving CO_2 in a nondispersive infrared (NDIR) detector. A_T was analyzed using an automated, open-cell potentiometric titration system developed and provided by A.Dickson (California, San Diego; Dickson et al. 2007). The accuracy and precision of the C_T and A_T measurements were verified using the certificated reference material - natural seawater obtained from the Marine Physical Laboratory, University of California, San Diego. The precision of the C_T and A_T measurements were ± 7 μmol kg^{-1} and ± 4 μmol kg^{-1}, respectively.

3.1.3. Calculations

C_T, A_T, salinity, temperature, and depth (pressure) were used as input parameters to the CO2SYS 2.1 software developed by Pierrot et al. (2006) to calculate pH, pCO_2, and the saturation state of aragonite (Ω_{Ar}). For calculations the following constants were used: the dissociation constants for carbonic acid estimated by Millero (2010), the HSO_4^- dissociation constant by Dickson (1990), and the borate dissociation constant from Uppström (1974). For pH values, the total hydrogen-ion scale was applied.

Freshwater fraction (FF) in samples was calculated using the following equation:

$$FF = 1 - \frac{S_{meas}}{S_{ref}} \quad (3)$$

where: S_{meas} is the measured S in the surface water sample; S_{ref} = 34.9, 34.9, and 34.5 (for Hornsund, Kongsfjorsden, and Krossfjorden, respectively), which are the mean S values measured in the water column (below the mixing layer) in this study.

For data visualization, Ocean Data View (Schlitzer, 2002) and ORIGIN 2021 Graphing & Analysis were used.

4. Results

4.1. Spatial distribution of S, T, A_T, C_T, pH, pCO_2 and Ω_{Ar}

Surface water S in the studied areas varied significantly - from 25.2 to 35.3 (Fig. 2). In Hornsund S ranged from 26.3 to 35.3, with the lowest results in two glacial bays - Brepollen and Burgerbukta (S < 30). S increased towards the mouth of the fjord, reaching the typical ocean values in the open part. In the Kongsfjorden-Krossfjorden system surface salinity was generally lower than in Hornsund, maximum values were 32.5 and 31.9, respectively. Lower S was found in the inner parts, which was especially pronounced in Kongsfjorden. In Krossfjorden salinity was also low, however, even in glacial bays (stations KrP.6, 7, and 10) it did not drop below 29. In the open part of the fjords S increased and the highest was measured at the Kb0 station. In Isfjorden S ranged from 31.2 to 33.1, however, the number of stations was lower there compared to other studied fjords, while side legs of Isfjorden where freshwater sources (rivers, glacier fronts) are located have not been sampled.

The surface T clearly divides the fjords into warmer and colder ones. Hornsund, where T ranged from 1.5 to 3.4 °C was significantly colder than other fjords. In the remaining fjords, the T ranged from 4.2 to 6.7 °C (Fig. 2).

Hydrography of the Spitsbergen fjords has been the subject of many publications (Pavlov et al., 2013; Promińska et al., 2017; Promińska et al., 2018; Skogseth et al., 2020), indicating a very large spatial and inter-annual variability of S in these areas, depending on the domination of the Sørkapp Current or the West Spitsbergen Current on the West Spitsbergen Shelf. Moreover, based on high-resolution CTD measurements collected between 2001 and 2015, Promińska et al. (2017) observed an increase in variability of temperature and salinity in recent years and generally strong influence of freshwater supply from land (rivers, melting glaciers) shaping S in the surface layer. This is confirmed with our results of S, which are in the range of previously reported data by Promińska et al. (2018) and Promińska et al. (2017).

Spatial distribution of alkalinity in surface waters was characterized by pronounced variability. The highest range was observed in Hornsund (1889–2261 μmol kg^{-1}), while the lowest in Isfjorden (2095–2189 μmol kg^{-1}; Fig. 2). Generally, the surface A_T followed salinity distribution with the lowest values found in the inner parts and glacial bays. It was especially pronounced in Kongsfjorden (most of the values below 2000 μmol kg^{-1}) and Hornsund (northern part of Brepollen). Obtained A_T results were (1) slightly lower (in particular in the lower range, probably due to the lower salinity) compared to the values previously reported for surface waters of the Svalbard fjords: 2130–2240 μmol kg^{-1} in Tempelfjorden (Fransson et al., 2015b), ~2060 μmol kg^{-1} in Adventfjorden (Ericson et al., 2019a), 2156–2303 μmol kg^{-1} in Kongsfjorden (results available for the central and inner part of the fjord only; Fransson et al., 2016) and (2) slightly higher (probably due to the higher salinity) than

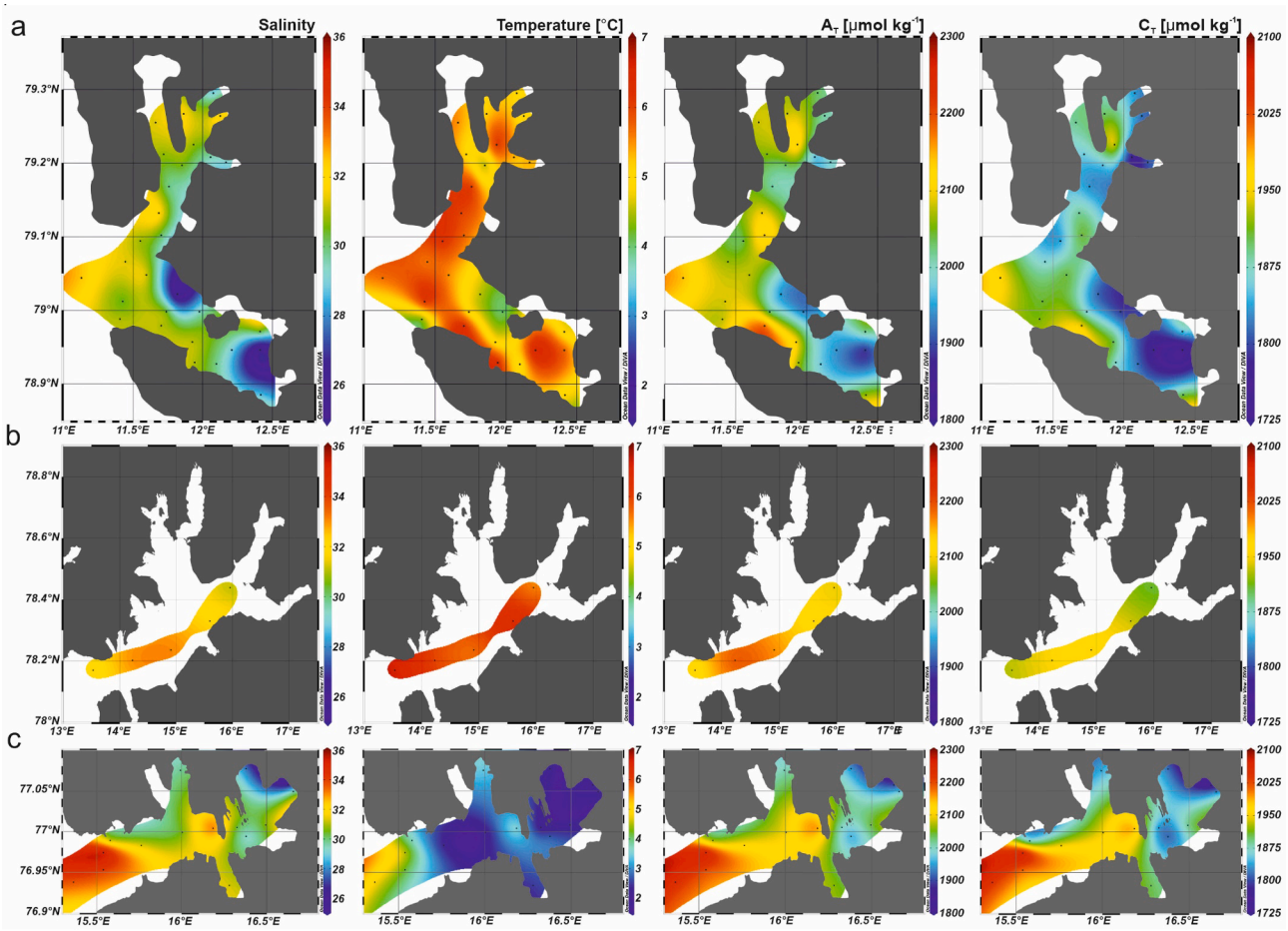

Fig. 2. Surface variability of salinity, temperature, A_T and C_T in the Krossfjorden and Kongsfjorden (a), Isfjorden (b) and Hornsund (c).

surface water minima ~1728 µmol kg^{-1} in 2016 and ~1593 µmol kg^{-1} in 2017 obtained by Ericson et al. (2015b) in Tempelfjorden. The A_T variability observed between the studies follows to a large extent the differences in salinity, which makes impossible to detect any regional or inter-annual trends.

The total inorganic carbon concentrations ranged from 1757 to 2065 µmol kg^{-1} in Hornsund, 1731 to 1957 µmol kg^{-1} in Kongsfjorden, 1779 to 1938 µmol kg^{-1} in Krossfjorden and 1910 to 1962 µmol kg^{-1} in Isfjorden (Fig. 2). C_T had similar spatial variability as A_T - in the open parts of the fjords C_T concentrations were significantly higher than closer to the land or glacier fronts. This dependence is particularly visible in Hornsund, where in the open part (station H1, HP.1 and HP.2) C_T was higher than 2200 µmol kg^{-1} and in the inner part (Brepollen Bay) it was lower than 2000 µmol kg^{-1}. Fransson et al. (2016) obtained comparable results, ranging from 1945 to 2064 µmol kg^{-1}, however, as for A_T, literature data are available only for the central and inner part of the Kongsfjorden.

In the investigated fjords pCO_2 ranged between 200 and 295 µatm (Fig. 3). In Hornsund, pCO_2 varied from 207 to 270 µatm, and its spatial variability along the fjord axis was minor compared to the glacial bays. The same pattern was observed for Krossfjorden, where results ranged from 200 to 265 µatm, with lower results observed closer to shore or in bays. Different pCO_2 spatial variability in surface water was observed in Kongsfjorden (212–295 µatm), with generally slightly higher results in the northwestern part, and lower pCO_2 in the southern and interior parts. In Isfjorden pCO_2 results ranged from 217 to 280 µatm. pH values in surface samples ranged from 8.13 to 8.29. The highest values have been estimated for Krossfjorden and especially for glacial bays. In Hornsund and Kongsfjorden pH was slightly lower (8.15–8.26 and 8.13–8.27, respectively). Generally, the pCO_2 and pH results are within the ranges previously observed for the Spitsbergen fjords. For instance, Fransson et al. (2016) based on the S, T, A_T, C_T, $[PO_4^{3-}]$ and $[Si(OH_4)]$ results calculated pH and fugacity of CO_2 (fCO_2) at few stations along the Kongsfjorden axis in 2013 and 2014. They found that pH in the upper 50 m layer oscillated in the ranges: 8.11–8.25 in 2013 and 8.22–8.28 in 2014, while fCO_2 in the surface layer (0–2 m) ranged from 197 to 305 µatm and from 192 to 235 µatm in 2013 and 2014, respectively. Fransson et al. (2016) used fCO_2 instead of pCO_2, however, the difference between these parameters is insignificant. fCO_2 is few µatm lower than pCO_2, because it accounts for the non-ideal nature of the gas phase (e.g. Dickson et al., 2007).

Aragonite saturation state in the studied area ranged between 1.4 and 2.5 (Fig. 3). Generally, the spatial variability of Ω_{Ar} was prominent. In Hornsund, higher values (up to 2.1) were found for the outer part and decreased towards the inner part of the fjord having its minimum (1.4) close to the glacier front in Brepollen. Significantly higher Ω_{Ar} variability, following high changes in pH, was observed in Kongsfjorden surface waters, where lower values were found in the northwestern part (minimum Ω_{Ar}: 1.5) and higher in the southern and inner parts (up to 2.5). Results in Krossfjorden ranged from 1.9 to 2.4, with higher results in the inner part of the fjord. In Isfjorden, Ω_{Ar} ranged from 2.0 to 2.5. Our results were generally lower than those obtained by Fransson et al. (2016) in 2014 in Kongsfjorden (Ω_{Ar} = 2.2–2.6), but within the range reported in the same study in 2013 in Kongsfjorden (Ω_{Ar} = 1.5–2.5), and Fransson et al. (2015b) and Ericson et al. (2019b) in Tempelfjorden.

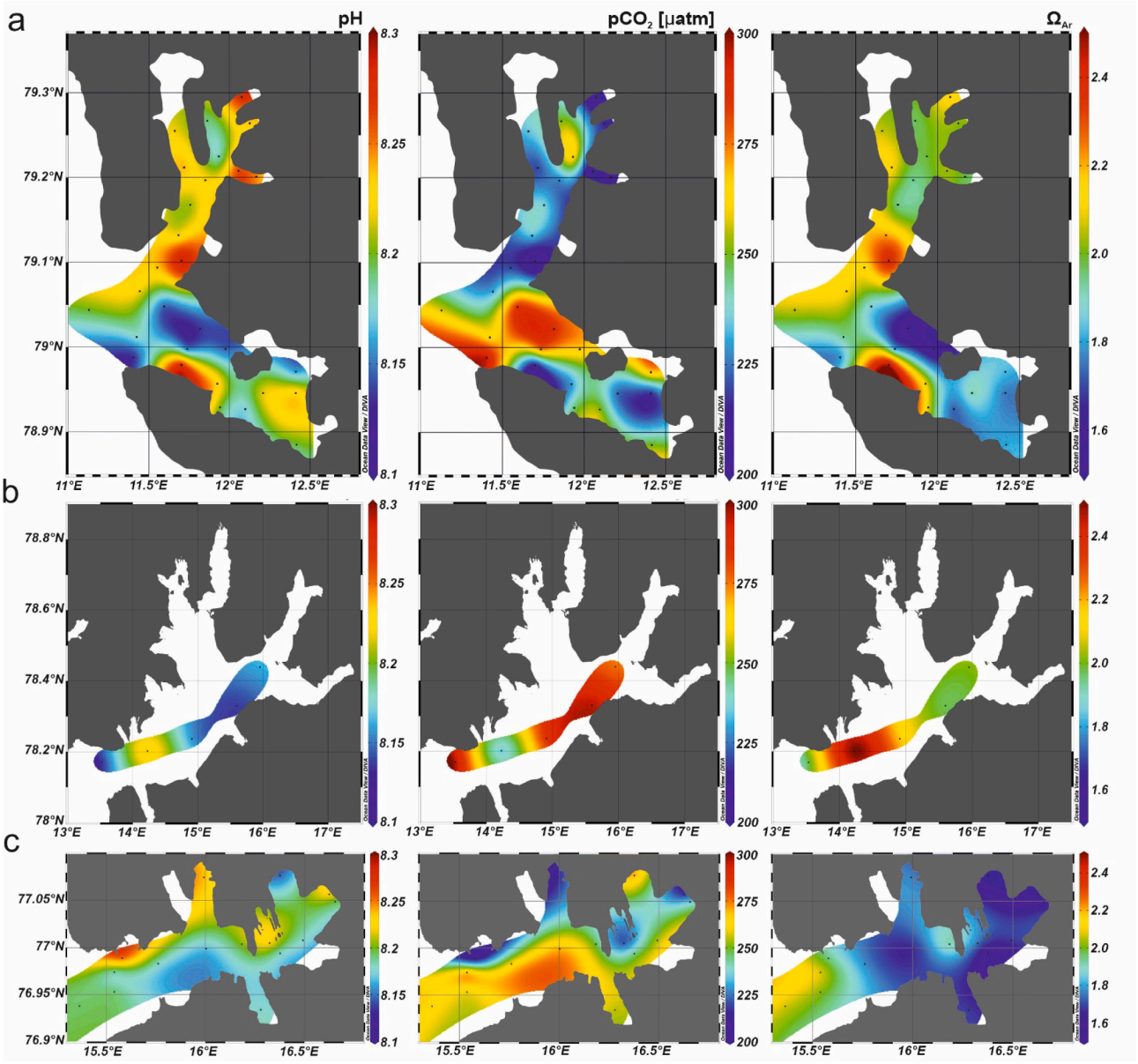

Fig. 3. Surface variability of pH, pCO_2 and ΩAr in the Krossfjorden and Kongsfjorden (a), Isfjorden (b) and Hornsund (c).

4.2. *Vertical distributions of S, T, A_T and C_T*

Vertical distribution of salinity at all sampling stations had the same pattern - high and relatively constant S, ~34.7, in the deep water column and its decrease in the surface layer due to mixing of seawater with freshwater originating from river runoff and meltwater from glaciers and sea ice (Svendsen et al., 2002) (Fig. A.1). However, the depth of the surface layer affected by the freshwater input was different in each fjord, in Hornsund it was found in the upper 35 m, in Kongsfjorden – 32 m, and Krossfjorden – 22 m. Moreover, the influence of freshwater was of varying intensity in different parts of the fjords. In Hornsund and Kongsfjorden S gradient between the surface and deeper water was clearly increasing towards the fjords' interiors. For instance in Hornsund, the S of the upper layer in the open part of the fjord was 33.7 and in the inner part was only 30.6, while S in the water column was very stable in whole fjord and ranged from 34.3 to 34.7. Stratification of water column is typical for Spitsbergen fjords. Promińska et al. (2018) based on long-term observations (2001–2015, except for 2004 and 2005) showed that the thickness of the surface layer during summer in Hornsund varied, from a few meters in 2014 to about 70 m in 2015.

The obtained T profiles clearly distinguish investigated fjords - Hornsund was colder than Kongsfjorden and Krossfjorden. In Hornsund, temperature ranged generally from 1.6 to 3.6 °C. The exception was station H4 located in Brepollen, where T below 50 m strongly decreased towards the bottom (below 0 °C). This is due to the occurrence of the sill separating deeper parts of Brepollen from the main basin (Promińska et al., 2018). The T in the surface layer in Kongsfjorden and Krossfjorden was much higher than in Hornsund, and the decrease with depth was also more pronounced (from 6.3 to 1.2 °C in Kongsfjorden and from 6.0 to 0.9 °C in Krossfjorden). This is due to the greater inflow of Atlantic Water and heat transport to both these fjords (Promińska et al., 2017). In the case of A_T and C_T results, a similar shape of vertical profiles as for S was observed – in the surface layer values of both parameters were significantly lower and more variable than in the deeper parts (Fig. A.1). A_T and C_T in the mixed layer ranged between 2044 and 2258 and

1890–2094 μmol kg^{-1} in Hornsund, 2067–2269 and 1905–2074 μmol kg^{-1} in Kongsfjorden and 2034–2273 and 1852–2093 μmol kg^{-1} in Krossfjorden, respectively. Below the mixing layer measured A_T and C_T values were very homogenous and ranged between 2279 and 2288 and 2092–2120 μmol kg^{-1} in Hornsund, 2274–2308 and 2031–2074 μmol kg^{-1} in Kongsfjorden and 2273–2302 and 2043–2102 μmol kg^{-1} in Krossfjorden, respectively. Ericson et al. (2019b) observed similar pattern during summer 2016 in Tempelfjorden - A_T and C_T was considerably diluted in the surface by the freshwater input, reaching minima of ~1728 μmol kg^{-1} and ~1593 μmol kg^{-1}, respectively, while, the deep water A_T and C_T values were ~2324 μmol kg^{-1} and ~2187 μmol kg^{-1}, respectively.

4.3. Pore water and sediment-overlying water salinity, A_T and C_T

Water samples collected 5 cm above the sediment surface were characterized by homogenous salinity at all stations (values ranged from 34.3 to 34.7; Table A1). In pore waters, however, salinity was generally slightly higher (except Kb1 station in the open part of Kongsfjorden), and much more variable (from 34.1 to 35.7). For A_T and C_T the discrepancies between values observed in sediment-overlying water and pore water were even larger. In the water above the sediment A_T was rather stable and ranged from 2277 to 2309 μmol kg^{-1}, while in pore waters it was significantly, even a few hundred micromoles, higher (2288–2666 μmol kg^{-1}). In the case of C_T, the concentrations in waters above the sediment ranged from 2057 to 2132 μmol kg^{-1} and were much lower from those found in pore waters which varied from 2106 to 3087 μmol kg^{-1} (the highest results found at the shallowest stations in Hornsund and Kongsfjorden). This clearly indicates that sediments in the studied fjords are the source of both A_T and C_T for the water column.

5. Discussion

Svalbard fjords form an important land–ocean continuum. Global warming has put them at the frontlines as particularly vulnerable regions, where new steep biogeochemical gradients are unfolding. Therefore, they can act as natural laboratories to investigate the impact of different stressors, such as increasing freshwater supply or decreasing sea ice extent on the marine CO_2 system structure and variability. Generally, inner parts of the fjords are more Arctic-type regions with less saline surface water layer influenced by freshwater input from land, and sometimes also with colder and more saline water in the deeper parts (so called winter cold water), that is created during sea ice formation, when the associated brine is released. While their outer parts are strongly influenced by water masses from the shelf – warmer and more saline Atlantic Water (AW) or cold Arctic Water (Hop et al., 2002). The studies by Promińska et al. (2018) and Promińska et al. (2017) showed that interannual variability in hydrography and water mass distribution in the studied Arctic fjords is immense. However, in 2018 the influence of AW was not very pronounced (Konsgfjorden and Krossfjorden), while the extend and gradient of less saline water were distinct, which gave an excellent opportunity to study the effect of freshwater - seawater mixing on the marine CO_2 system variability and alkalinity distribution in particular.

5.1. Alkalinity anomalies

Total alkalinity is often considered a conservative parameter in seawater chemistry, which changes along with salinity. The first major attempt to examine correlations of alkalinity with other more commonly measured hydrographic parameters was made for the North Atlantic Ocean by Brewer et al. (1995). Next, Millero et al. (1998) presented extensive research on the surface A_T measurements of the major ocean basins (Atlantic, Pacific, and Indian Oceans; $A_T = 51.24S + 520.1$). Since that time, a significant number of new surface water A_T measurements have been added to the global data set, thus further estimates to determine the relationships of A_T with S for different regions have been made (e.g. Friis et al., 2003; Lee et al., 2006; Cai et al., 2010; Jiang et al., 2014; Takahashi et al., 2014). Compared to the relatively simple situation in the open ocean, coastal waters can involve more complex processes regulating A_T distribution. These regions are usually strongly influenced by multiple freshwater sources (rivers, melting glaciers), which may have different A_T concentrations depending on the processes occurring in the catchment and its geological structure. Moreover processes occurring in the water column like calcification, $CaCO_3$ dissolution, or brine formation play a significant role in controlling A_T distribution in the coastal regions. In addition to that, alkalinity release from sediments has been also suggested as key driver shaping the A_T budget (Fig. 4) (Chen and Wang, 1999; Chen, 2002; Thomas et al., 2009; Fennel, 2010; Lukawska-Matuszewska and Graca, 2018).

5.1.1. Effect of freshwater supply on surface water layer

Surface water in fjords is influenced by both vertical mixing within the water column and horizontal mixing with open ocean water and freshwater from various sources - glacier ablation, ice melting, river runoff and precipitation. To investigate the effects of freshwater supply, the surface water layer (SWL) was defined in this study according to the classification of water masses with respect to ranges in temperature and salinity found for Spitsbergen fjords by Nilsen et al. (2008): $T > 1$ °C and $S < 34$. This classification will be used throughout Sections 5.1-5.3.

A decline in A_T is evident with decreasing salinity which suggests

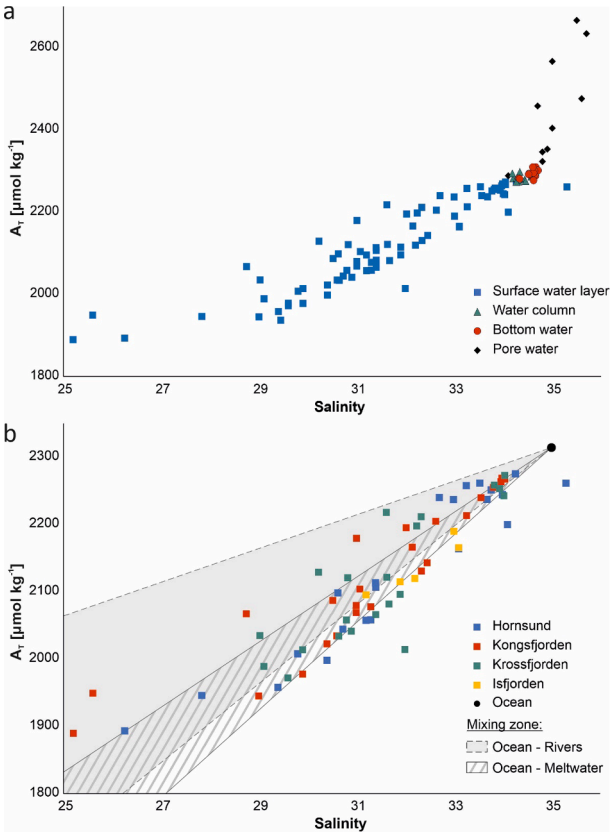

Fig. 4. Crossplots between A_T and S results for (a) SWL, water column, bottom water and pore water, and (b) SWL only, which was defined according to the classification by Nilsen et al. (2008). Lines and marked ranges indicate dilution of typical Ocean Water (S = 35 and mean $A_T = 2315 \pm 2$ μmol kg^{-1} calculated based on A_T vs S dependence provided by Millero et al. (1998), Lee et al. (2006) and Takahashi et al. (2014)) with freshwater having A_T ranges defined as: Rivers (S = 0 and A_T from 232 to 1412 μmol kg^{-1}) and Meltwater (S = 0 and A_T from 0 to 600 μmol kg^{-1}). The A_T ranges for Rivers and Meltwater were determined based on available literature data for polar regions (presented in Table 1).

Table 1
Freshwater alkalinity end-member obtained in this study compared with other polar regions.

Region	A_T [μmol kg^{-1}]	Comments*	Data source**	Reference
S Alaska	430	–	measured	Anderson et al. (2000)
Laptev Sea	1412	–	measured	Anderson et al. (2004)
Arctic rivers	~1048	–	measured	Cooper et al. (2008)
Young Sound	269–440	–	measured	Sejr et al. (2011)
SE Beaufort Sea	797	–	extrapolated	Shadwick et al. (2011)
Greenland	242–670	–	measured	Rysgaard et al. (2012a)
Bering Sea shelf	1244	–	measured	Cross et al. (2013)
East GIN Seas	232	$A_T + NO_3^-$	extrapolated	Takahashi et al. (2014)
Tempelfjorden	1142	III and IV 2012	extrapolated	Fransson et al. (2015b)
	526	September 2013	extrapolated	
	0–378	–	measured	
SW Greenland	50 ± 20	–	measured	Meire et al. (2015)
Cumberland Sound (Canada)	175–600	–	measured	Turk et al. (2016)
			measured	
W Fram Strait	1230	–	extrapolated	Tynan et al. (2016)
Nordic Seas	403	–	extrapolated	
Adventdalen	243 ± 3	–	measured	Ericson et al. (2018)
Tempelfjorden	355 ± 24	2016	extrapolated	Ericson et al. (2019b)
	601 ± 42	2017	extrapolated	
Canadian Arctic Archipelago	648	–	extrapolated	Mears et al. (2020)
W Spitsbergen	595 ± 84	–	extrapolated	This study

* specific information: season, year.
** direct measurements of freshwater or calculated based on extrapolating the A_T vs S relationship to S = 0.

generally lower alkalinity concentrations in freshwater (Fig. 4). However, SWL was also characterized by a pronounced variability of A_T and its partial decoupling from salinity, which may indicate: (1) multiple freshwater sources of different A_T end-member values (Cooper et al., 2008; Takahashi et al., 2014; Tynan et al., 2016) and/or (2) occurrence of processes that can affect A_T without changing salinity - calcification, $CaCO_3$ dissolution, primary production, respiration (Wolf-Gladrow et al. 2007) and/or (3) occurrence of process that influence both A_T and S but cause also decoupling between both – processes related to sea ice formation and melting e.g. $CaCO_3$ precipitation within the sea ice and thus rejection of A_T-depleted brine, and the release of excess A_T during ice melt (Rysgaard et al., 2007; Fransson et al., 2015b).

Riverine alkalinity end-member depends mainly on the characteristics of its catchment (geological structure, land cover or vegetation structure). Literature data indicate a wide range of values in the polar regions (Table 1). For instance, Cooper et al. (2008) found average A_T end-member for six Arctic largest rivers to be ~ 1048 μmol kg^{-1}, in Adventdalen (W Spitsbergen) freshwater alkalinity was 243 ± 3 μmol kg^{-1} (Ericson et al., 2018). However, rivers are not the only source of freshwater in the polar regions as there is also a direct inflow of meltwater from glaciers for which A_T range from 0 to 600 μmol kg^{-1} (Anderson et al., 2000; Sejr et al., 2011; Rysgaard et al., 2012a; Fransson et al., 2015a; Meire et al., 2015; Turk et al., 2016). The multitude of freshwater sources that affect the SWL, as well as still insufficient identification of their A_T end-member values in the Spitsbergen fjords, make the interpretation of the variability of alkalinity and, consequently of the entire CO_2 system, intricate.

As it is shown in Fig. 4b, the bulk of surface A_T results (595 ± 84 μmol kg^{-1}) fall within the areas bounded by the dilution lines drawn between typical Ocean Water (S = 35 and mean A_T = 2315 ± 2 μmol kg^{-1}) and either meltwater (S = 0 and A_T between 0 and ~ 600 μmol kg^{-1}) or river water (S = 0 and A_T from 232 to 1412 μmol kg^{-1}) – both these A_T ranges for freshwater have been identified based on available literature data for polar regions (presented in Table 1). A number of glaciers located on Spitsbergen cause that meltwater enters the fjords either directly (glaciers calving) or feeds rivers. This results in a high contribution of meltwater in the freshwater budget and explains that most of the obtained A_T results follow the mixing pattern between ocean water and meltwater. However, some A_T values, for example from Kongsfjorden and Krossfjorden, are higher than it would appear from meltwater influence only (Fig. 4b). This may be due to the bedrock characteristics of the fjord's catchment, which is largely composed of carbonate rocks (i.a. marbles, dolomite, limestone, silicide carbonate). Weathering, but also abrasion and glaciers calving may deliver carbonates to coastal zone either in dissolved or in particulate form (Martin and Meybeck, 1979). The dissolved fraction (bicarbonate and/or carbonate ions) contributes directly to A_T budget. Particles may be deposited to marine sediments, without effect on A_T, or dissolved adding to A_T pool. Carbonate mineral species, such as dolomite are characterized by lower solubility than calcite (Middelburg, 2019). Thus, both the quantity and quality of the particulate carbonates is crucial for their further influence on the seawater alkalinity. Koziorowska et al. (2017) estimated that the concentration of particulate carbonates (PIC) in proximity to the Kronebeen glacier (Kongsfjorden) is much higher (0.19–0.75 mg dm^{-3}) than in the central and open parts of the fjord (0.01–0.07 mg dm^{-3}). Inorganic carbon concentration was also high in surface sediments (up to 45.5 mg g^{-1}) and authors estimated that glaciers were its main source. D'Angelo et al. (2018) measured high export to sediments of total particulate matter in the inner part of Kongsfjorden, with the highest peak (330 g m^{-2} d^{-1}) during summer. Particles mainly consisted of siliciclastic material, and carbonates were the second most abundant component (18.4–31.5%). The authors also emphasized that shells of living carbonatic organisms were not the main source of particulate carbonates but they likely originated from the clastic sediment delivered by Kronebreen and Kongsvegen glaciers. Unfortunately, none of these publications (Koziorowska et al., 2017; D'Angelo et al., 2018) clearly indicates the further fate of PIC in seawater. Probably it is mostly accumulated in sediments (high concentrations), however it is not known how much PIC may dissolve in seawater and thus contribute to A_T. The high variability in bedrock geology (presence of carbonate vs non-carbonate rocks) may explain the elevated surface alkalinity in some regions, as well as its high variability throughout the fjords. The processes that can also significantly influence A_T are the formation and melting of sea ice. $CaCO_3$ precipitate in the form of ikaite crystals within the sea ice cause release of A_T-depleted brine. During sea ice melting, dissolution of ikaite trapped in the ice matrix may cause enrichment of

surface waters with excess A_T. Fransson et al. (2015a) stated that in Kongsfjorden, apart from the changes due to salinity and brine rejection, the concentrations of C_T, A_T and CO_2 in melted ice were influenced by the dissolution of calcium carbonate precipitates (25–55 μmol kg^{-1}). This study looked at the wintertime, however, Rysgaard et al. (2012a) showed that in summer, dissolution of the minerals during melting of the sea ice can considerably influence the carbonate system of surface water, for example, measured pH in melting sea ice was 9.9–10.1, significantly higher than the pH of the surface water layer (pH = 8.3–8.4). Moreover, Chierici et al. (2019) calculated that in August in the eastern Fram Strait and north area of Svalbard, a C_T gain caused by shells and/or ikaite dissolution (and thus also an increase in A_T) ranged from 0.2 mol C m^{-2} in shelf and meltwater influenced domain to 0.7 mol C m^{-2} in the Atlantic water domain.

On the other hand, some A_T results, were below the line describing mixing of ocean water with the freshwater of $A_T = 0$ (Fig. 4b). This may be the effect of processes depleting water in A_T such as calcification and/or respiration (Wolf-Gladrow et al., 2007). The latter, however, has rather minor influence on A_T, which additionally in surface water is compensated by counteracting effect of primary production. On the other hand, calcification has a great potential to affect A_T as along with one mole of $CaCO_3$ formed two moles of A_T are removed. Generally, calcifying phytoplankton blooms occur after the spring bloom and organisms can usually sustain growth during summer, but this is not often seen in the Arctic Ocean (Tyrrell and Merico, 2004). A key calcyfing species of Arctic pelagic ecosystems is free-swimming pteropod mollusc *Limacina helicina*, often located in swarms or forming aggregates in surface waters (0–50 m) (Kobayashi, 1974). However, literature data indicate its importance in the zooplankton community structure rather in Kongsfjorden than in Hornsund waters, as its biomass increases with temperature and salinity (Blachowiak-Samolyk et al., 2008; Ormanczyk et al., 2017).

This study provides a unique and comprehensive database and significantly improves our knowledge about A_T distribution in the west Spitsbergen fjords. It reveals the complexity of the fjords' systems with multiple freshwater sources having different A_T end-member characteristics. Although it is clear that freshwater input with a mean A_T of 595 ± 84 μmol kg^{-1} (Fig. 4b) generally has a diluting effect and lowers A_T in the surface waters of the Spitsbergen fjords, full deciphering and biogeochemical characterization of individual freshwater end-members is impossible based on the present database. This is due to both the multitude of freshwater sources and a complex hydrological setting in this tidal region. Furthermore, we believe that the increase of A_T observations in these fjords may not necessarily guarantee that the tangled relationship between A_T and S would be unravelled. To do that, it would be necessary to construct an A_T budget that would take into account both the end-member A_T concentrations of individual freshwater sources and their water flows, which would allow estimating of reliable flow-weighted A_T end-member concentrations for individual fjords. However, even without such a detailed approach, the database presented in this study provides an important insight into the structure and variability of the marine CO_2 system in the high Arctic fjords during the high meltwater season and consists of a reference for future studies in the region.

5.1.2. Sediments as a source of alkalinity

Marine sediments can also play an important role in shaping alkalinity, as some of the OM remineralization processes that occur during early diagenesis lead to the A_T release (Berner et al., 1970). Aerobic remineralization of OM including nitrification of the produced ammonium act as an A_T sink, while anaerobic remineralization processes (e.g. denitrification, manganese, iron and sulphate reduction) in general produce A_T (Brenner et al., 2016). However, as most of these redox reactions are reversible, the reduced forms are oxidized when conditions turn back to oxic, which makes the net effect for alkalinity is zero. This is not the case for denitrification during which nonreactive N_2 is produced and A_T release is permanent. Similarly, the positive net effect for A_T balance is sustained when the reduced form of Fe is buried in the course of pyrite and/or vivianite formation (Gustafsson et al., 2019). In addition, low pH occurring usually in sediments may lead to $CaCO_3$ dissolution and thus A_T release (Brenner et al., 2016).

In the present study, A_T was much higher in pore waters than in the sediment overlying waters (Fig. 4a), which indicates sediments as a potential source of alkalinity to the water column. In Kongsfjorden, important role may play dissolution of carbonates, which are deposited in large amounts in the surface sediments (concentration from 17 to 45 mg g^{-1}) (Koziorowska et al., 2017). In Hornsund, much lower carbonate concentrations (<10 mg g^{-1}) and higher organic matter content in the sediments could suggest higher importance of OM mineralization processes (Koziorowska et al., 2018). However, in both fjords, large differences in A_T:C_T ratios (0.86–1.16 and 0.93–1.15, respectively) would indicate the interaction of various processes on the A_T values in the pore waters. Higher increase of A_T than C_T indicates the occurrence of processes such as iron reduction, or $CaCO_3$ dissolution, while lower A_T:C_T ratio – denitrification (slightly lower increase of A_T than C_T), aerobic oxidation of OM (slight decrease of A_T and C_T production) or processes that decrease only A_T and C_T stays constant (e.g. oxidation of ammonia, hydrogen sulphide) (Krumins et al., 2013). Brenner et al. (2016) estimated sediment fluxes of A_T ranging from 0 to 28.7 mmol m^{-2} d^{-1} in the North Sea, suggesting that OM remineralization is the primary driver for the A_T release from sediments. Chen and Wang (1999) quantified that the East China Sea sediments can produce between 2.9 and 4.9 mmol m^{-2} d^{-1} of A_T due to iron and sulfate reduction. Gustafsson et al. (2019) estimated A_T release of 2.4 mmol m^{-2} d^{-1} from the Baltic Sea sediments, with denitrification as the main source. On the other hand, Miller et al. (2017) measured A_T flux for deep sediments of East Siberian slope (between the Mendeleev and the Lomonosov ridges) to be only 0.005–0.04 mmol m^{-2} d^{-1}, which confirms that the influence of sediments in open oceans is much smaller than in the coastal regions. In this respect it is still unclear how important can be sedimentary A_T generation in the Arctic fjords. Although the obtained results do not allow for quantification of the net A_T release, they clearly show the potential of sediments in the Spitsbergen fjords as a source of A_T (Fig. 4a). This mechanism may add to the A_T variability and thus also to the complexity of the entire marine CO_2 system in the region and as such it requires more detailed studies.

5.2. Influence of increasing freshwater supply on saturation state of $CaCO_3$ in the surface water layer

The saturation state of calcite and aragonite is an important chemical indicator, which informs, if solid $CaCO_3$ is chemically unstable and prone to dissolution ($\Omega < 1$). It is also commonly used to demonstrate the biological consequences of Ocean Acidification, as calcifying organisms have shown to have difficulty in shell formation, and thinning of the shells was observed in already living organisms at lower saturation states (Comeau et al., 2009; Bednarsek and Ohman, 2015). Although the thermodynamic undersaturation is defined for $\Omega < 1$, the recent publications have suggested that aragonite forming calcifying organisms may have problems even at $\Omega > 1$. For instance, for free-swimming pelagic pteropod mollusc *Limacina helicina* this threshold was found for 1.4 (Lischka et al., 2011; Bednarsek et al., 2014). Generally, increasing freshwater fraction (FF) reduces seawater A_T (Fig. 5a). Even if the catchment is rich in carbonate rocks, the riverine A_T end-members are lower (~1400 μmol kg^{-1} according to available data for polar regions; Table 1) than seawater A_T and consequently, inflow of freshwater from land lowers A_T in the coastal zone. The FF in the surface water layer of studied fjords ranged from − 2 to 24% (one negative value results from higher salinity in the sample than the assumed reference salinity for this fjord, S_{ref} − 34.49) in Hornsund, 4–10% in Isfjorden, 1–27% in Kongsfjorden and 1–16% in Krossfjorden. Fig. 5a clearly shows that freshwater discharge reduces A_T and therefore reduces the aragonite saturation state. This general conclusion is evident though

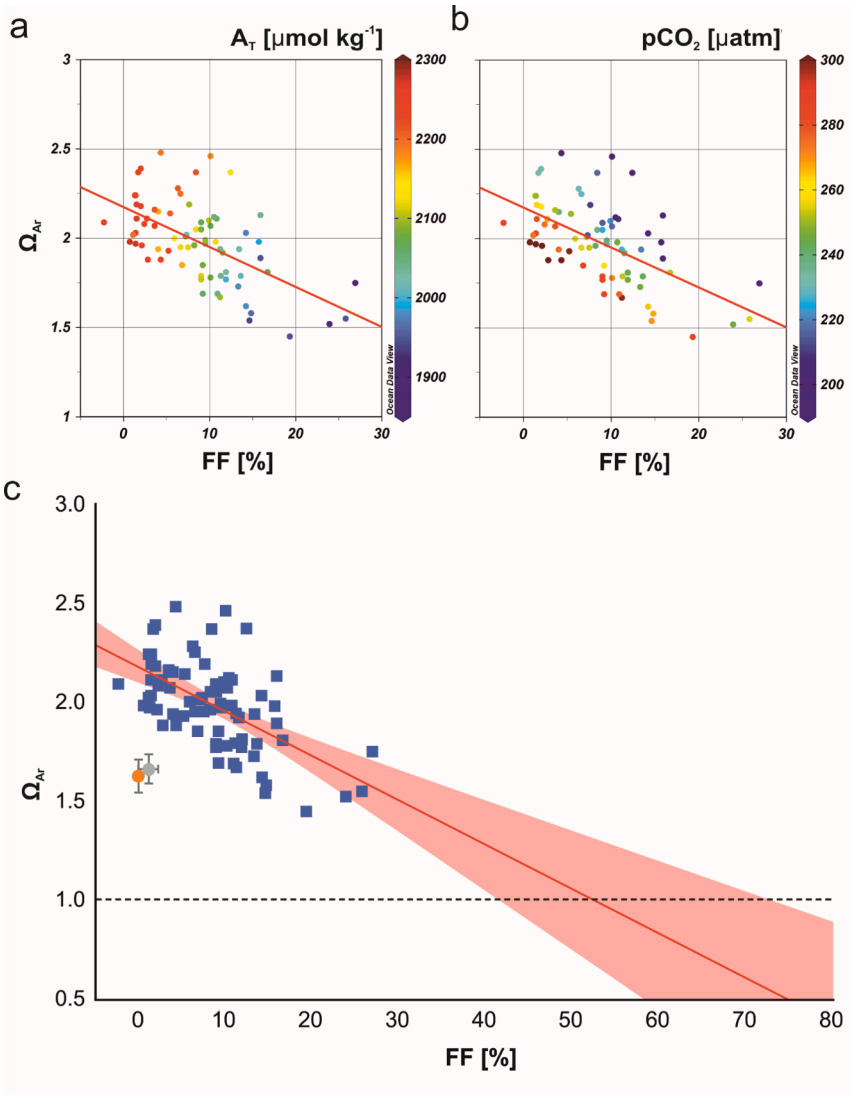

Fig. 5. Ω_{Ar} as a function of freshwater fraction (FF) contribution and alkalinity (a) and pCO_2 (b) in the surface water layer (all results normalized to a constant temperature of 4.3 °C; the red line shows a linear trend). (c) Ω_{Ar} as a function of FF contribution, blue dots - values obtained in this study (normalized to a constant T = 4.3 °C), orange and grey dots – mean Ω_{Ar} values calculated assuming: A_T values obtained in this study with FF contribution lower than 2% (orange dot) and A_T values from the water column (below the mixing layer) obtained in this study (grey dot), pCO_2 = 370 µatm (an annual maximum) and temperature equal to −0.9 °C – the latter two measured by Fransson et al. (2015b) in winter (March) in Tempelfjorden. Red line indicate linear regression, pink fields indicate 95%, confidence band.

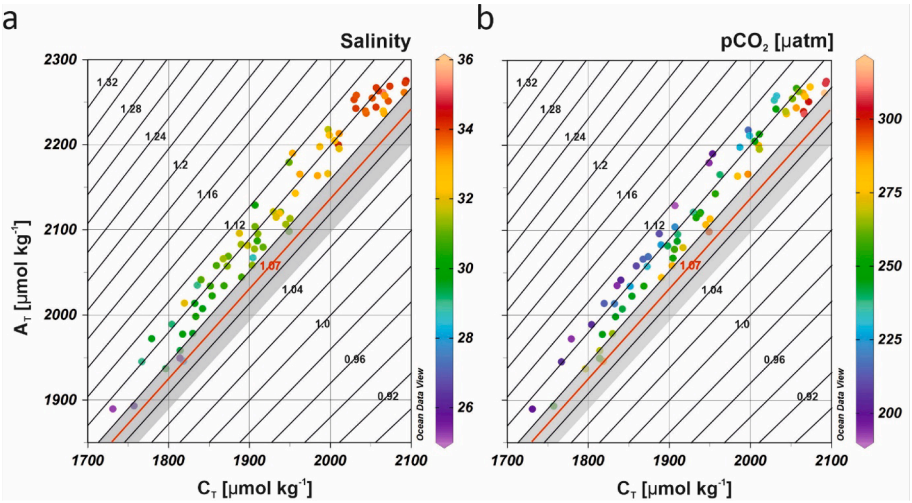

Fig. 6. The crossplot of A_T and C_T in the SWL with a range of colour denoting salinity (a) and pCO_2 normalized for constant temperature of 4.3 °C (b). The isolines indicate the A_T to C_T ratios. Grey fields represent the range of A_T:C_T values calculated for winter conditions, and the red lines show the mean of these values.

high spread of the results suggests high heterogeneity of the A_T freshwater end-members. As Ω_{Ar} is also affected by the temperature, the average T = 4.3 °C was used for all the calculations to unravel the influence of FF on Ω_{Ar}. The linear regression for dependency between Ω_{Ar} and FF has a negative slope of − 0.022, which means that an increase in FF by 1% causes a decrease in Ω_{Ar} by 0.022. This is slightly lower slope than − 0.032 ± 0.003 and − 0.028 ± 0.001 found in 2016 and 2017 in Tempelfjorden by Ericson et al. (2019b), but higher than − 0.009 estimated by Ericson et al. (2019a) for Adventfjorden. Based on this regression, it can be also calculated that the increase in freshwater fraction to 41–73% (mean value = 52%) will make the water in fjords undersaturated with respect to aragonite (Fig. 5c). This estimation assumes that our results are representative for summer period and other processes such as primary production or air-sea CO_2 exchange remain unchanged. Climate warming causes freshening of fjords' waters which may result in Ω_A reduction. Blaszczyk et al. (2019) found that 2517 ± 82 Mt year^{-1} of freshwater inflow to Hornsund (mean for the period 2006–2015), out of which the highest contribution constitutes meltwater runoff 39% and frontal ablation 25%. In addition to FF, Ω_{Ar} can also be modified by primary production and respiration, both having opposing effects. As CO_2 is taken up during photosynthesis, pCO_2 decreases, while pH and $[CO_3^{2-}]$ and thus also Ω increase. This is well seen in Fig. 5b where despite the increase in FF and decrease in A_T, Ω_{Ar} remains high along with low pCO_2. The lowest pCO_2 values in this study were mostly found in surface waters in the glacial bays close to the glacier front (especially in Krossfjorden and Hornsund), which may suggest the positive influence of glacial freshwater discharge on primary production. Generally, discharge of freshwater from melting glaciers is associated with the local suppression of primary production, due to e.g. the high stratification, particulate flux, turbidity, or light limitation (Hopwood et al., 2020). However, marine-terminating glaciers can increase summertime primary production by the enhanced vertical mixing in water column, which increases macronutrients availability (Gerringa et al., 2012; Meire et al., 2015; Hopwood et al., 2020). However, the positive effect of freshwater supply on primary production is not the only potential explanation for the lower pCO_2 values in glacial bays. Recently, many authors pointed out other processes that can explain low pCO_2 in the inner parts of the fjords, which is commonly observed in Arctic fjords (Sejr et al., 2011; Rysgaard et al., 2012b; Meire et al., 2015; Torres et al., 2017). First explanation indicates, that meltwater itself can be undersaturated with CO_2 and thus its inflow may reduce pCO_2 of seawater. However, Meire et al. (2015) found that this effect has minor importance. Moreover, they proposed a different explanation suggesting that it can be the thermodynamic effect on the surface water pCO_2 resulting from the mixing of fresh glacial meltwater and ambient saline fjord water. Regardless of the process that is responsible for the reduction of pCO_2 in the seawater in the inner part of the fjords, this indicates that the freshwater supply can both lower Ω_{Ar} through a decrease in A_T, as well as increase it through a decrease in pCO_2 (and thus increase in pH and $[CO_3^{2-}]$). However, all these observations refer to the summer period when the pCO_2 values in the surface water are low (in Tempelfjorden, Ericson et al. (2019b) found the lowest values in April-June and Fransson et al. (2015b) in September), and the freshwater supply is high. During the winter time, pCO_2 values increase significantly (no primary production, respiration is the dominant process). Fransson et al. (2015b) measured maximim 370 µatm in mid-March and Ericson et al. (2019b) 330 µatm in the late March. Although this shows that seawater was undersaturated with CO_2 throughout the year, the increase of pCO_2 in wintertime can significantly affect Ω_{Ar}. To simulate the scale of this effect we calculated theoretical Ω_{Ar} values for the winter period. This was done by using as the input data: (1) the A_T values measured in our study with FF contribution lower than 2% and (2) A_T values from the water column (below the mixing layer) obtained in this study and winter time pCO_2 = 370 µatm and temperatures (–1.6 to –0.3 °C, mean T = –0.9 °C) – both reported by Fransson et al. (2015b) for Tempelfjorden (Fig. 5c). The alkalinity values (1 and 2) used for the calculations were chosen to best reflect the conditions that can be observed in winter in these areas (e.g. wind-induced convection with deep water, negligible freshwater fraction contribution). Although this theoretical exercise is undoubtedly burdened with uncertainty, it clearly shows that an increase of pCO_2 during wintertime may significantly lower Ω_{Ar} to 1.6–1.7. This calculation emphasizes that good recognition of the processes that shape the structure of the marine CO_2 system and its variability (including seasonality) is necessary for understanding and predicting consequences of climate changes on the Arctic fjords ecosystems.

5.3. A_T:C_T ratio as an indicator of biogeochemical processes

To determine which biogeochemical processes are responsible for shaping the marine CO_2 system, the crossplots between A_T and C_T, with pCO_2 and pH as an additional variable are often used (Middelburg, 2019; Middelburg et al., 2020). In this study, the A_T:C_T ratios ranged from 1.07 to 1.12 (average ± SD = 1.10 ± 0.01) in the surface water layer, and did not change significantly with salinity, and thus also with the distance from the coast and glaciers or rivers (freshwater sources; Fig. 6a). The results were in a similar range to those found for shelf areas of Southern Greenland (Rysgaard et al., 2012b), but rather in the upper range of the A_T:C_T ratios reported for e.g. Bering Sea or Canadian Arctic

Archipelago (Azetsu-Scott et al., 2010). This may indicate that the surface seawater in the Spitsbergen fjords was either slightly enriched with A_T, or depleted in C_T, or both, compared to the regions described by Azetsu-Scott et al. (2010). Generally, low pCO_2 values and their clear negative correlation with A_T:C_T ratios (the lower pCO_2 the higher A_T:C_T, Fig. 6b) suggests net community production (primary production minus ecosystem respiration) and air-sea CO_2 exchange as the main drivers of changes in A_T:C_T ratios. In addition to C_T decrease, primary production leads also to a small A_T increase, which corresponds to H^+ uptake equivalent to assimilation of nitrates. To estimate the influence of net community production on A_T:C_T ratios the C_T values measured in our study have been subtracted from those representing winter conditions, which have been calculated in a similar way to the presented in chapter 5.2, namely out of the measured A_T and pCO_2 of 370 μatm measured by Fransson et al. (2015b) in March in Tempelfjorden. Determined in that way a cumulative C_T loss (ΔC_T) caused by net community production (cumulative means without gas exchange; NCP-gasex) amounts to 30–90 μmol kg^{-1}. In accordance with the Redfield ratio (Redfield et al., 1963), this cumulative C_T loss corresponds to A_T increase of 4–14 μmol kg^{-1}. This, in total, causes that the winter A_T:C_T ratio would oscillate at about 1.05–1.08 (average ± SD = 1.07 ± 0.01; red line and grey area in Fig. 6a and b). This ΔC_T, refers to the period of about 136–149 days, which is the time between our sampling and winter time pCO_2 measurements made by Fransson et al. (2015b) on March 12. Assuming that mean thickness of the euphotic zone is about 20 m (range from 1 m to 35 m for 1% of photosynthetically active radiation in Hornsund and Kongsfjorden) (Smoła et al., 2017) the NCP-gasex for the studied area ranged from 0.09 to 0.13 g C m^{-2} day^{-1}. The NCP was certainly higher, however, the inability to estimate CO_2 gas exchange in the corresponding period did not allow us for its quantification. Literature data indicate that waters in the west Spitsbergen coast are significant CO_2 sink. Józefiak et al. (2021) found that they absorb on average ~ 30 g C m^{-2} y^{-1}, while Ericson et al. (2019b) calculated that the mean uptake of CO_2 in Tempelfjorden between June and early August was 0.19 g m^{-2} day^{-1}.

6. Conclusions

Arctic fjords give an excellent opportunity to study the effect of seawater freshening related to ongoing global warming and resulting from that glaciers retreat on the marine CO_2 system. Inner parts of the fjords are more Arctic type regions with less saline surface waters due to freshwater input from land, while outer parts are strongly influenced by ocean water masses from the open shelf. These differences were clearly visible in the variability of surface salinity, especially in Hornsund, where the influence of more saline water (up to 35.3) from the shelf was the most pronounced. The differences in hydrology entail spatial changes in the CO_2 system structure. In the case of alkalinity, a decline with decreasing salinity was evident, hence it is clear that freshwater input generally has a diluting effect and lowers A_T in the surface waters of the Spitsbergen fjords. However, the relationship between A_T and S was highly heterogeneous. It reveals the complexity of the fjords' systems with multiple freshwater sources having different A_T end-member characteristics and identifies the mean A_T freshwater end-member of 595 ± 84 μmol kg^{-1} for the entire region. Low pCO_2 results in surface water (200–295 μatm) indicates occurrence of intensive biological production. The latter can strongly affect C_T values, however, is less important for shaping alkalinity. The effect of A_T fluxes from sediments on the bottom water was rather insignificant, despite high A_T values (2288–2666 μmol kg^{-1}) observed in the pore waters at most of the stations. The lack of clear relationship between A_T and salinity indicates that the use of salinity and temperature to estimate the potential alkalinity of seawater can carry a high uncertainty in the highly dynamic Arctic coastal regions. It has been shown that the freshening of the surface water layer in the fjords reduces significantly Ω_{Ar}. Based on our data, an increase in freshwater fraction contribution by 1% causes a decrease in Ω_{Ar} by 0.022, while the FF of 41–73% makes the water undersaturated for aragonite (assuming that other processes, such as primary production or air-sea CO_2 exchange, remain unchanged). Although in summer Ω_{Ar} values are still rather far from 1 (they ranged from 1.4 to 2.5), during winter, when pCO_2 values are much higher, Ω_{Ar} may drop markedly.

This study provides an important insight into the structure of the marine CO_2 system in the high Arctic fjords during the high meltwater season and highlights that good recognition of the surface water A_T variability and its freshwater end-members are the key to predict marine CO_2 system changes along with the ongoing freshening of fjords waters due to climate warming.

Declaration of Competing Interest

The authors declare that they have no known competing financial interests or personal relationships that could have appeared to influence the work reported in this paper.

Data availability

Data will be made available on request.

Acknowledgements

This study was financially supported by the National Science Centre, Poland (2019/34/E/ST10/00167), the Norwegian Financial Mechanism 2014–2021 (85%) National Science Centre (15%) within GRIEG Programme (2019/34/H/ST10/00645 and 2019/34/H/ST10/00504), and Helmholtz-Zentrum Hereon, Institute of Carbon Cycles, Geesthacht, Germany. Katarzyna Koziorowska-Makuch acknowledges the scholarship in the frame of Bekker Programme (PPN/BEK/2019/1/00070) funded by the Polish National Agency for Academic Exchange. Helmuth Thomas acknowledges support from the German Academic Exchange service (DAAD, MOPGA-GRI, grant no. 57429828), which received funds from the German Federal Ministry of Education and Research (BMBF).

Appendix

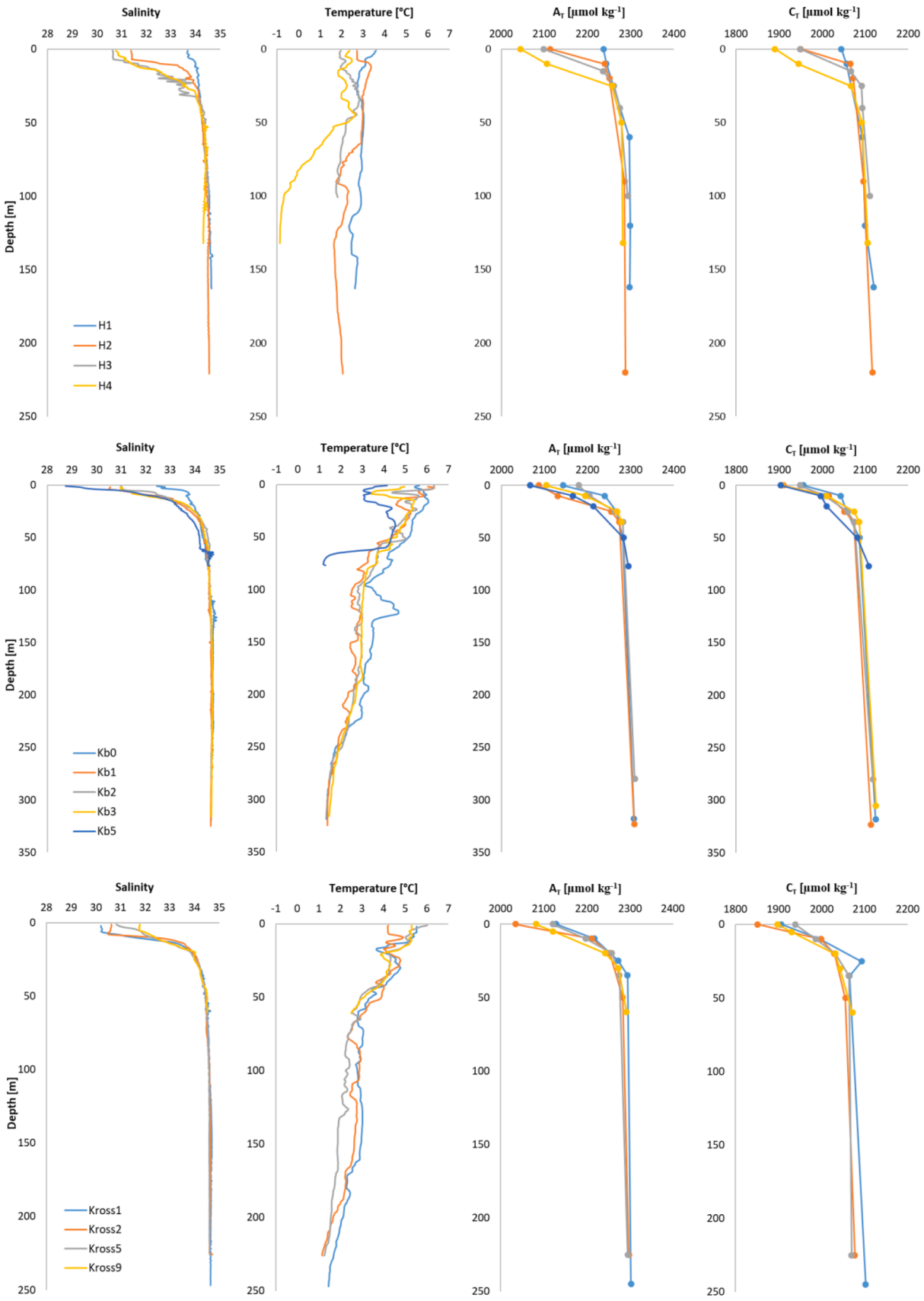

Fig. A1. Vertical distributions of salinity, temperature, A_T, C_T in Hornsund (upper panel), Kongsfjorden (middle panel) and Krossfjorden (lower panel).

Table A1
Results of S, A_T, C_T in pore water and sediment-overlying water.

Station	Type	Depth	Salinity	A_T [μmol/kg]	C_T [μmol/kg]
H1	above the sediment	164	34.7	2306	2115
	pore water	–	–	–	–
H2	above the sediment	227	34.5	2290	2113
	pore water	227.3	34.7	2458	2139
H3	above the sediment	107	34.5	2291	2107
	pore water	107.3	35.0	2404	2582
H4	above the sediment	136	34.3	2281	2100
	pore water	136.3	35.0	2566	
Kb0	above the sediment	326	34.7	2301	2031
	pore water	–	–	–	–
Kb1	above the sediment	325	34.7	2307	2110
	pore water	325.3	34.1	2288	2114
Kb2	above the sediment	282	34.7	2288	2100
	pore water	282.3	35.7	2634	2279
Kb3	above the sediment	315	34.7	2292	2098
	pore water	315.3	34.9	2353	2285
Kb5	above the sediment	83	34.7	2291	2109
	pore water	83.3	35.5	2666	3087
Kross1	above the sediment	281	34.7	2301	2079
	pore water	281.3	35.6	2476	2240
Kross2	above the sediment	243	34.6	2300	2133
	pore water	243.3	35.0	–	2270
Kross5	above the sediment	230	34.6	2309	2074
	pore water	230.3	34.8	2346	2132
Kross9	above the sediment	65	34.6	2277	2057
	pore water	65.3	34.8	2323	2106

References

Anderson, S.P., Drever, J.I., Frost, C.D., Holden, P., 2000. Chemical weathering in the foreland of a retreating glacier. Geochim. Cosmochim. Acta 64, 1173–1189. https://doi.org/10.1016/S0016-7037(99)00358-0.

Anderson, L.G., Jutterstrom, S., Kaltin, S., Jones, E.P., Bjork, G.R., 2004. Variability in river runoff distribution in the Eurasian Basin of the Arctic Ocean. J. Geophys. Res. Oceans 109. https://doi.org/10.1029/2003jc001773.

Azetsu-Scott, K., Clarke, A., Falkner, K., Hamilton, J., Jones, E.P., Lee, C., Petrie, B., Prinsenberg, S., Starr, M., Yeats, P., 2010. Calcium carbonate saturation states in the waters of the Canadian Arctic Archipelago and the Labrador Sea. J. Geophys. Res. Oceans 115. https://doi.org/10.1029/2009jc005917.

Bates, N.R., Mathis, J.T., 2009. The Arctic Ocean marine carbon cycle: evaluation of air-sea CO2 exchanges, ocean acidification impacts and potential feedbacks. Biogeosciences 6, 2433–2459. https://doi.org/10.5194/bg-6-2433-2009.

Bednarsek, N., Ohman, M.D., 2015. Changes in pteropod distributions and shell dissolution across a frontal system in the California Current System. Mar. Ecol. Prog. Ser. 523, 93–103. https://doi.org/10.3354/meps11199.

Bednarsek, N., Tarling, G.A., Bakker, D.C.E., Fielding, S., Feely, R.A., 2014. Dissolution Dominating Calcification Process in Polar Pteropods Close to the Point of Aragonite Undersaturation. PLoS One 9, e109183.

Berner, R.A., Scott, M.R., Thomlinson, C., 1970. Carbonate alkalinity in the pore water of anoxic marine sediments. Limnol. Oceanogr. 15, 544–549. https://doi.org/10.4319/lo.1970.15.4.0544.

Beszczyńska-Moller, A., Węsławski, J.M., Walczowski, W., Zajączkowski, M., 1997. Estimation of glacial meltwater discharge into Svalbard coastal waters. Oceanologia 39 (3), 289–298.

Bianchi, T.S., Arndt, S., Austin, W.E.N., Douglas, I.B., Bertrand, S., Cui, X.Q., Faust, J.C., Koziorowska-Makuch, K., Moy, C.M., Savage, C., Smeaton, C., Smith, R.W., Syvitski, J., 2020. Fjords as Aquatic Critical Zones (ACZs). Earth Sci. Rev. 203, 103145 https://doi.org/10.1016/j.earscirev.2020.103145.

Blachowiak-Samolyk, K., Soreide, J.E., Kwasniewski, S., Sundfjord, A., Hop, H., Falk-Petersen, S., Hegseth, E.N., 2008. Hydrodynamic control of mesozooplankton abundance and biomass in northern Svalbard waters (79–81 degrees N). Deep-Sea Research Part Ii-Topical Studies in Oceanography 55, 2210–2224. https://doi.org/10.1016/j.dsr2.2008.05.018.

Blaszczyk, M., Ignatiuk, D., Uszczyk, A., Cielecka-Nowak, K., Grabiec, M., Dania, J. A., Moskalik, M., Walczowski, W., 2019. Freshwater input to the Arctic fjord Hornsund (Svalbard). Polar Research 38. 10.33265/polar.v38.3506.

Blaszczyk, M., Jania, J.A., Kolondra, L., 2013. Fluctuations of tidewater glaciers in Hornsund Fjord (Southern Svalbard) since the beginning of the 20th century. Polish Polar Research 34, 327–352. https://doi.org/10.2478/popore-2013-0024.

Brenner, H., Braeckman, U., Le Guitton, M., Meysman, F.J.R., 2016. The impact of sedimentary alkalinity release on the water column CO2 system in the North Sea. Biogeosciences 13, 841–863. https://doi.org/10.5194/bg-13-841-2016.

Brewer, P.G., Glover, D.M., Goyet, C., Shafer, D.K., 1995. The pH of the North-Atlantic Ocean - Improvements to the global-model for sound-absorption in seawater. J. Geophys. Res. Oceans 100, 8761–8776. https://doi.org/10.1029/95jc00306.

Cai, W.J., Hu, X.P., Huang, W.J., Jiang, L.Q., Wang, Y.C., Peng, T.H., Zhang, X., 2010. Alkalinity distribution in the western North Atlantic Ocean margins. J. Geophys. Res. Oceans 115, C08014. https://doi.org/10.1029/2009jc005482.

Carmack, E.C., Yamamoto-Kawai, M., Haine, T.W.N., Bacon, S., Bluhm, B.A., Lique, C., Melling, H., Polyakov, I.V., Straneo, F., Timmermans, M.L., Williams, W.J., 2016. Fresh water and its role in the Arctic Marine System: Sources, disposition, storage, export, and physical and biogeochemical consequences in the Arctic and global oceans. J. Geophys. Res. Biogeo. 121, 675–717. https://doi.org/10.1002/2015JG003140.

Chen, C.T.A., 2002. Shelf-vs. dissolution-generated alkalinity above the chemical lysocline. Deep-Sea Research Part Ii-Topical Studies in Oceanography 49, 5365–5375. https://doi.org/10.1016/s0967-0645(02)00196-0.

Chen, C.T.A., Wang, S.L., 1999. Carbon, alkalinity and nutrient budgets on the East China Sea continental shelf. J. Geophys. Res. Oceans 104, 20675–20686. https://doi.org/10.1029/1999jc900055.

Chierici, M., Vernet, M., Fransson, A., Borsheim, K.Y., 2019. Net Community Production and Carbon Exchange From Winter to Summer in the Atlantic Water Inflow to the Arctic Ocean. Front. Mar. Sci. 6 https://doi.org/10.3389/fmars.2019.00528.

Comeau, S., Gorsky, G., Jeffree, R., Teyssie, J.L., Gattuso, J.P., 2009. Impact of ocean acidification on a key Arctic pelagic mollusc (Limacina helicina). Biogeosciences 6, 1877–1882. https://doi.org/10.5194/bg-6-1877-2009.

Cooper, L.W., McClelland, J.W., Holmes, R.M., Raymond, P.A., Gibson, J.J., Guay, C.K., Peterson, B.J., 2008. Flow-weighted values of runoff tracers (delta 18O, DOC, Ba, alkalinity) from the six largest Arctic rivers. Geophys. Res. Lett. 35 https://doi.org/10.1029/2008gl035007.

Cross, J.N., Mathis, J.T., Bates, N.R., Byrne, R.H., 2013. Conservative and non-conservative variations of total alkalinity on the southeastern Bering Sea shelf. Mar. Chem. 154, 100–112. https://doi.org/10.1016/j.marchem.2013.05.012.

Dallmann, W.K., Ohta, Y., Elvevold, S., Blomeier, D., 2002. Bedrock map of Svalbard and Jan Mayen. Norsk Polarinstitutt Temakart 33.

D'Angelo, A., Giglio, F., Miserocchi, S., Sanchez-Vidal, A., Aliani, S., Tesi, T., Viola, A., Mazzola, M., Langone, L., 2018. Multi-year particle fluxes in Kongsfjorden, Svalbard. Biogeosciences 15, 5343–5363. https://doi.org/10.5194/bg-15-5343-2018.

Dickson, A.G., 1981. An exact definition of total alkalinity and a procedure for the estimation of alkalinity and total inorganic carbon from titration data. Deep-Sea Research Part a-Oceanographic Research Papers 28, 609–623. https://doi.org/10.1016/0198-0149(81)90121-7.

Dickson, A.G., 1990. Standard potential of the reaction - AgCl(s)+12H2(g)=Ag(s)+HCl(aq) and the standard acidity constant of the ion HSO4- in synthetic sea-water from 273.15K to 318.15K. J. Chem. Thermodyn. 22, 113–127. https://doi.org/10.1016/0021-9614(90)90074-z.

Dickson, A.G., Sabine, C.L., Christian, J.R., 2007. Guide to Best Practices for Ocean CO2 Measurements. Sidney, BC Canada.

Ericson, Y., Chierici, M., Falck, E., Fransson, A., Jones, E., Kristiansen, S., 2019a. Seasonal dynamics of the marine CO2 system in Adventfjorden, a west Spitsbergen fjord. Polar Research 38. 10.33265/polar.v38.3345.

Ericson, Y., Falck, E., Chierici, M., Fransson, A., Kristiansen, S., Platt, S.M., Hermansen, O., Myhre, C.L., 2018. Temporal Variability in Surface Water pCO(2) in Adventfjorden (West Spitsbergen) With Emphasis on Physical and Biogeochemical

Drivers. J. Geophys. Res. Oceans 123, 4888–4905. https://doi.org/10.1029/2018jc014073.
Ericson, Y., Falck, E., Chierici, M., Fransson, A., Kristiansen, S., 2019b. Marine CO2 system variability in a high arctic tidewater-glacier fjord system, Tempelfjorden, Svalbard. Cont. Shelf Res. 181, 1–13. https://doi.org/10.1016/j.csr.2019.04.013.
Fennel, K., 2010. The role of continental shelves in nitrogen and carbon cycling: Northwestern North Atlantic case study. Ocean Science 6, 539-548. 10.5194/os-6-539-2010.
Fransson, A., Chierici, M., Abrahamsson, K., Andersson, M., Granfors, A., Gardfeldt, K., Torstensson, A., Wulff, A., 2015a. CO2-system development in young sea ice and CO2 gas exchange at the ice/air interface mediated by brine and frost flowers in Kongsfjorden, Spitsbergen. Ann. Glaciol. 56, 245–257. https://doi.org/10.3189/2015AoG69A563.
Fransson, A., Chierici, M., Nomura, D., Granskog, M.A., Kristiansen, S., Martma, T., Nehrke, G., 2015b. Effect of glacial drainage water on the CO2 system and ocean acidification state in an Arctic tidewater-glacier fjord during two contrasting years. J. Geophys. Res. Oceans 120, 2413–2429. https://doi.org/10.1002/2014jc010320.
Fransson, A., Chierici, M., Hop, H., Findlay, H.S., Kristiansen, S., Wold, A., 2016. Late winter-to-summer change in ocean acidification state in Kongsfjorden, with implications for calcifying organisms. Polar Biol. 39, 1841–1857. https://doi.org/10.1007/s00300-016-1955-5.
Fransson, A., Chierici, M., Nomura, D., Granskog, M.A., Kristensen, D.K., Martma, T., Nehrke, G., 2020. Influence of glacial water and carbonate minerals on wintertime sea-ice biogeochemistry and the CO2 system in an Arctic fjord in Svalbard. Ann. Glaciol. 1–21 https://doi.org/10.1017/aog.2020.52.
Friis, K., Kortzinger, A., Wallace, D.W.R., 2003. The salinity normalization of marine inorganic carbon chemistry data. Geophys. Res. Lett. 30, 1085. https://doi.org/10.1029/2002gl015898.
Gazeau, F., Quiblier, C., Jansen, J.M., Gattuso, J.P., Middelburg, J.J., Heip, C.H.R., 2007. Impact of elevated CO2 on shellfish calcification. Geophys. Res. Lett. 34 https://doi.org/10.1029/2006gl028554.
Gerringa, L.J.A., Alderkamp, A.C., Laan, P., Thuroczy, C.E., De Baar, H.J.W., Mills, M.M., van Dijken, G.L., van Haren, H., Arrigo, K.R., 2012. Iron from melting glaciers fuels the phytoplankton blooms in Amundsen Sea (Southern Ocean): Iron biogeochemistry. Deep-Sea Research Part Ii-Topical Studies in Oceanography 71–76, 16–31. https://doi.org/10.1016/j.dsr2.2012.03.007.
Gustafsson, E., Hagens, M., Sun, X.L., Reed, D.C., Humborg, C., Slomp, C.P., Gustafsson, B.G., 2019. Sedimentary alkalinity generation and long-term alkalinity development in the Baltic Sea. Biogeosciences 16, 437–456. https://doi.org/10.5194/bg-16-437-2019.
Hagen, J., 1993. Glacier atlas of Svalbard and Jan Mayen. Norsk Polarinstitutt Middelelser.
Holmes, F.A., Kirchner, N., Kuttenkeuler, J., Krutzfeldt, J., Noormets, R., 2019. Relating ocean temperatures to frontal ablation rates at Svalbard tidewater glaciers: Insights from glacier proximal datasets. Sci. Rep. 9 https://doi.org/10.1038/s41598-019-45077-3.
Hop, H., Pearson, T., Hegseth, E.N., Kovacs, K.M., Wiencke, C., Kwaśniewski, S., Eiane, K., Mehlum, F., Gulliksen, B., Włodarska-Kowalczuk, M., Lydersen, C., Węsławski, J.M., Cochrane, S., Gabrielsen, G.W., Leakey, R.J.G., Lonne, O.J., Zajączkowski, M., Falk-Petersen, S., Kendall, M., Wangberg, S.A., Bischof, K., Voronkov, A.Y., Kovaltchouk, N.A., Wiktor, J., Poltermann, M., di Prisco, G., Papucci, C., Gerland, S., 2002. The marine ecosystem of Kongsfjorden, Svalbard. Polar Res. 21, 167–208. https://doi.org/10.1111/j.1751-8369.2002.tb00073.x.
Hopwood, M.J., Carroll, D., Dunse, T., Hodson, A., Holding, J.M., Iriarte, J.L., Ribeiro, S., Achterberg, E.P., Cantoni, C., Carlson, D.F., Chierici, M., Clarke, J.S., Cozzi, S., Fransson, A., Juul-Pedersen, T., Winding, M.H.S., Meire, L., 2020. Review article: How does glacier discharge affect marine biogeochemistry and primary production in the Arctic? Cryosphere 14, 1347–1383. https://doi.org/10.5194/tc-14-1347-2020.
Husum, K., Howe, J. A., Baltzer, A., Forwick, M., Jensen, M., Jernas, P., Korsun, S., Miettinen, A., Mohan, R., Morigi, C., Myhre, P. I., Prins, M. A., Skirbekk, K., Sternal, B., Boos, M., Dijkstra, N., Troelstra, S., 2019. The marine sedimentary environments of Kongsfjorden, Svalbard: an archive of polar environmental change. Polar Research 38. 10.33265/polar.v38.3380.
IPCC, 2019: Summary for Policymakers. In: Climate Change and Land: an IPCC special report on climate change, desertification, land degradation, sustainable land management, food security, and greenhouse gas fluxes in terrestrial ecosystems [P.R. Shukla, J. Skea, E. Calvo Buendia, V. Masson-Delmotte, H.- O. Pörtner, D. C. Roberts, P. Zhai, R. Slade, S. Connors, R. van Diemen, M. Ferrat, E. Haughey, S. Luz, S. Neogi, M. Pathak, J. Petzold, J. Portugal Pereira, P. Vyas, E. Huntley, K. Kissick, M. Belkacemi, J. Malley, (eds.)]. In press.
Jiang, Z.P., Tyrrell, T., Hydes, D.J., Dai, M.H., Hartman, S.E., 2014. Variability of alkalinity and the alkalinity-salinity relationship in the tropical and subtropical surface ocean. Global Biogeochem. Cycles 28, 729–742. https://doi.org/10.1002/2013gb004678.
Józefiak, I., Santana, Y., Müller, L., Ordóñez, C., Donis, D., Mcginnis, D. 2021. Greenhouse gas fluxes (CO2 and CH4) in the Arctic Ocean: results from the sailboat Mauritius.*in* ASLO 2021.
Kim, H., Kwon, S.Y., Lee, K., Lim, D., Han, S., Kim, T.W., Joo, Y.J., Lim, J., Kang, M.H., Nam, S.I., 2020. Input of terrestrial organic matter linked to deglaciation increased mercury transport to the Svalbard fjords. Sci. Rep. 10, 3446. https://doi.org/10.1038/s41598-020-60261-6.
Kobayashi, H.A., 1974. Growth-cycle and related vertical distribution of the thecosomatous pteropod Spiratella (Limacina) Helicina in central Arctic Ocean. Mar. Biol. 26, 295–301. https://doi.org/10.1007/bf00391513.
Koziorowska, K., Kuliński, K., Pempkowiak, J., 2017. Distribution and origin of inorganic and organic carbon in the sediments of Kongsfjorden, Northwest Spitsbergen, European Arctic. Cont. Shelf Res. 150, 27–35. https://doi.org/10.1016/j.csr.2017.08.023.
Koziorowska, K., Kuliński, K., Pempkowiak, J., 2018. Comparison of the burial rate estimation methods of organic and inorganic carbon and quantification of carbon burial in two high Arctic fjords. Oceanologia. https://doi.org/10.1016/j.oceano.2018.02.005.
Krumins, V., Gehlen, M., Arndt, S., Van Cappellen, P., Regnier, P., 2013. Dissolved inorganic carbon and alkalinity fluxes from coastal marine sediments: model estimates for different shelf environments and sensitivity to global change. Biogeosciences 10, 371–398. https://doi.org/10.5194/bg-10-371-2013.
Le Quere, C., Andrew, R.M., Friedlingstein, P., Sitch, S., Hauck, J., Pongratz, J., Pickers, P.A., Korsbakken, J.I., Peters, G.P., Canadell, J.G., Arneth, A., Arora, V.K., Barbero, L., Bastos, A., Bopp, L., Chevallier, F., Chini, L.P., Ciais, P., Doney, S.C., Gkritzalis, T., Goll, D.S., Harris, I., Haverd, V., Hoffman, F.M., Hoppema, M., Houghton, R.A., Hurtt, G., Ilyina, T., Jain, A.K., Johannessen, T., Jones, C.D., Kato, E., Keeling, R.F., Goldewijk, K.K., Landschutzer, P., Lefevre, N., Lienert, S., Liu, Z., Lombardozzi, D., Metzl, N., Munro, D.R., Nabel, J., Nakaoka, S., Neill, C., Olsen, A., Ono, T., Patra, P., Peregon, A., Peters, W., Peylin, P., Pfeil, B., Pierrot, D., Poulter, B., Rehder, G., Resplandy, L., Robertson, E., Rocher, M., Rodenbeck, C., Schuster, U., Schwinger, J., Seferian, R., Skjelvan, I., Steinhoff, T., Sutton, A., Tans, P.P., Tian, H.Q., Tilbrook, B., Tubiello, F.N., van der Laan-Luijkx, I.T., van der Werf, G.R., Viovy, N., Walker, A.P., Wiltshire, A.J., Wright, R., Zaehle, S., Zheng, B., 2018. Global Carbon Budget 2018. Earth Syst. Sci. Data 10, 2141–2194. https://doi.org/10.5194/essd-10-2141-2018.
Lee, K., Tong, L.T., Millero, F.J., Sabine, C.L., Dickson, A.G., Goyet, C., Park, G.H., Wanninkhof, R., Feely, R.A., Key, R.M., 2006. Global relationships of total alkalinity with salinity and temperature in surface waters of the world's oceans. Geophys. Res. Lett. 33 https://doi.org/10.1029/2006gl027207.
Li, W. K. W., McLaughlin, F. A., Lovejoy, C., Carmack, E. C., 2009. Smallest Algae Thrive As the Arctic Ocean Freshens. Science 326, 539-539. 10.1126/science.1179798.
Lischka, S., Budenbender, J., Boxhammer, T., Riebesell, U., 2011. Impact of ocean acidification and elevated temperatures on early juveniles of the polar shelled pteropod Limacina helicina: mortality, shell degradation, and shell growth. Biogeosciences 8, 919–932. https://doi.org/10.5194/bg-8-919-2011.
Lukawska-Matuszewska, K., Graca, B., 2018. Pore water alkalinity below the permanent halocline in the Gdansk Deep (Baltic Sea) - Concentration variability and benthic fluxes. Mar. Chem. 204, 49–61. https://doi.org/10.1016/j.marchem.2018.05.011.
Maclachlan, S.E., Howe, J.A., Vardy, M.E., 2011. Morphodynamic evolution of Kongsfjorden-Krossfjorden, Svalbard, during the Late Weichselian and Holocene. In: Howe, J.A., Austin, W.E.N., Forwick, M., Paetzal, M. (Eds.), Fjord Systems and Archives. Geological Society London Special Publications, pp. 195–205.
Martin, J.M., Meybeck, M., 1979. Elemental mass-balance of material carried by major world rivers. Mar. Chem. 7, 173–206. https://doi.org/10.1016/0304-4203(79)90039-2.
Mears, C., Thomas, H., Henderson, P.B., Charette, M.A., MacIntyre, H., Dehairs, F., Monnin, C., Mucci, A., 2020. Using Ra-226 and Ra-228 isotopes to distinguish water mass distribution in the Canadian Arctic Archipelago. Biogeosciences 17, 4937–4959. https://doi.org/10.5194/bg-17-4937-2020.
Meire, L., Sogaard, D.H., Mortensen, J., Meysman, F.J.R., Soetaert, K., Arendt, K.E., Juul-Pedersen, T., Blicher, M.E., Rysgaard, S., 2015. Glacial meltwater and primary production are drivers of strong CO2 uptake in fjord and coastal waters adjacent to the Greenland Ice Sheet. Biogeosciences 12, 2347–2363. https://doi.org/10.5194/bg-12-2347-2015.
Meredith, M., M. Sommerkorn, S. Cassotta, C. Derksen, A. Ekaykin, A. Hollowed, G. Kofinas, A. Mackintosh, J. Melbourne-Thomas, M.M.C. Muelbert, G. Ottersen, H. Pritchard, and E.A.G. Schuur, 2019: Polar Regions. In: IPCC Special Report on the Ocean and Cryosphere in a Changing Climate [H.-O. Pörtner, D.C. Roberts, V. MassonDelmotte, P. Zhai, M. Tignor, E. Poloczanska, K. Mintenbeck, A. Alegría, M. Nicolai, A. Okem, J. Petzold, B. Rama, N.M. Weyer (eds.)]. In press.
Middelburg, J. J., Soetaert, K., Hagens, M., 2020. Ocean Alkalinity, Buffering and Biogeochemical Processes. Reviews of Geophysics 58 (3), e2019RG000681. 10.1029/2019RG000681.
Middelburg, J. J. 2019. Biogeochemical Processes and Inorganic Carbon Dynamics. Pages 76-105 Marine Carbon Biogeochemistry A Primer for Earth System Scientists. Springer.
Miller, C.M., Dickens, G.R., Jakobsson, M., Johansson, C., Koshurnikov, A., O'Regan, M., Muschitiello, F., Stranne, C., Morth, C.M., 2017. Pore water geochemistry along continental slopes north of the East Siberian Sea: inference of low methane concentrations. Biogeosciences 14, 2929–2953. https://doi.org/10.5194/bg-14-2929-2017.
Millero, F.J., 2010. Carbonate constants for estuarine waters. Mar. Freshw. Res. 61, 139–142. https://doi.org/10.1071/mf09254.
Millero, F.J., Lee, K., Roche, M., 1998. Distribution of alkalinity in the surface waters of the major oceans. Mar. Chem. 60, 111–130. https://doi.org/10.1016/s0304-4203(97)00084-4.
Nilsen, F., Cottier, F., Skogseth, R., Mattsson, S., 2008. Fjord-shelf exchanges controlled by ice and brine production: The interannual variation of Atlantic Water in Isfjorden, Svalbard. Cont. Shelf Res. 28, 1838–1853. https://doi.org/10.1016/j.csr.2008.04.015.
Ormanczyk, M.R., Gluchowska, M., Olszewska, A., Kwasniewski, S., 2017. Zooplankton structure in high latitude fjords with contrasting oceanography (Hornsund and Kongsfjorden, Spitsbergen). Oceanologia 59, 508–524. https://doi.org/10.1016/j.oceano.2017.06.003.

Pavlov, A.K., Tverberg, V., Ivanov, B.V., Nilsen, F., Falk-Petersen, S., Granskog, M.A., 2013. Warming of Atlantic Water in two west Spitsbergen fjords over the last century (1912–2009). Polar Res. 32, 11206. https://doi.org/10.3402/polar.v32i0.11206.

Pierrot, D. E., Lewis, E., Wallace, D. W. R. 2006. MS Excel Program Developed for CO2 System Calculations. ORNL/CDIAC-105a. Carbon Dioxide Information Analysis Center, Oak Ridge National Laboratory, U.S. Department of Energy, Oak Ridge, Tennessee.

Promińska, A., Cisek, M., Walczowski, W., 2017. Kongsfjorden and Hornsund hydrography - comparative study based on a multiyear survey in fjords of west Spitsbergen. Oceanologia 59, 397–412. https://doi.org/10.1016/j.oceano.2017.07.003.

Promińska, A., Falck, E., Walczowski, W., 2018. Interannual variability in hydrography and water mass distribution in Hornsund, an Arctic fjord in Svalbard. Polar Res. 37, 1495546. https://doi.org/10.1080/17518369.2018.1495546.

Redfield, A.C., Ketchum, B.H., Richards, F.A., 1963. The Influence of Organisms on the Composition of the Sea Water. In: Hill, M.N. (Ed.), The Sea. Interscience Publishers, New York, pp. 26–77.

Rysgaard, S., Glud, R.N., Sejr, M.K., Bendtsen, J., Christensen, P.B., 2007. Inorganic carbon transport during sea ice growth and decay: A carbon pump in polar seas. J. Geophys. Res. Oceans 112. https://doi.org/10.1029/2006jc003572.

Rysgaard, S., Glud, R.N., Lennert, K., Cooper, M., Halden, N., Leakey, R.J.G., Hawthorne, F.C., Barber, D., 2012a. Ikaite crystals in melting sea ice - implications for pCO(2) and pH levels in Arctic surface waters. Cryosphere 6, 901–908. https://doi.org/10.5194/tc-6-901-2012.

Rysgaard, S., Mortensen, J., Juul-Pedersen, T., Sorensen, L.L., Lennert, K., Sogaard, D.H., Arendt, K.E., Blicher, M.E., Sejr, M.K., Bendtsen, J., 2012b. High air-sea CO2 uptake rates in nearshore and shelf areas of Southern Greenland: Temporal and spatial variability. Mar. Chem. 128, 26–33. https://doi.org/10.1016/j.marchem.2011.11.002.

Schlitzer, R., 2002. Interactive analysis and visualization of geoscience data with Ocean Data View. Comput. Geosci. 28, 1211–1218. https://doi.org/10.1016/s0098-3004(02)00040-7.

Schuur, E.A.G., McGuire, A.D., Schadel, C., Grosse, G., Harden, J.W., Hayes, D.J., Hugelius, G., Koven, C.D., Kuhry, P., Lawrence, D.M., Natali, S.M., Olefeldt, D., Romanovsky, V.E., Schaefer, K., Turetsky, M.R., Treat, C.C., Vonk, J.E., 2015. Climate change and the permafrost carbon feedback. Nature 520, 171–179. https://doi.org/10.1038/nature14338.

Sejr, M.K., Krause-Jensen, D., Rysgaard, S., Sorensen, L.L., Christensen, P.B., Glud, R.N., 2011. Air-sea flux of CO2 in arctic coastal waters influenced by glacial melt water and sea ice. Tellus Series B-Chemical and Physical Meteorology 63, 815–822. https://doi.org/10.1111/j.1600-0889.2011.00540.x.

Shadwick, E.H., Thomas, H., Chierici, M., Else, B., Fransson, A., Michel, C., Miller, L.A., Mucci, A., Niemi, A., Papakyriakou, T.N., Tremblay, J.E., 2011. Seasonal variability of the inorganic carbon system in the Amundsen Gulf region of the southeastern Beaufort Sea. Limnol. Oceanogr. 56, 303–322. https://doi.org/10.4319/lo.2011.56.1.0303.

Shadwick, E.H., Trull, T.W., Thomas, H., Gibson, J.A.E., 2013. Vulnerability of Polar Oceans to Anthropogenic Acidification: Comparison of Arctic and Antarctic Seasonal Cycles. Sci. Rep. 3 https://doi.org/10.1038/srep02339.

Skogseth, R., Olivier, L.L.A., Nilsen, F., Falck, E., Fraser, N., Tverberg, V., Ledang, A.B., Vader, A., Jonassen, M.O., Soreide, J., Cottier, F., Berge, J., Ivanov, B.V., Falk-Petersen, S., 2020. Variability and decadal trends in the Isfjorden (Svalbard) ocean climate and circulation - An indicator for climate change in the European Arctic. Prog. Oceanogr. 187 https://doi.org/10.1016/j.pocean.2020.102394.

Smoła, Z., Tatarek, A., Wiktor, J., Wiktor Jr., J., Hapter, R., Kubiszyn, A., Węsławski, J. M., 2017. Primary producers and production in two West Spitsbergen fjords (Hornsund and Kongsfjorden) – a review. Polish Polar Resarch 38 (3), 351–373. https://doi.org/10.1515/popore-2017-0013.

Streuff, K., 2013. Landform assemblages in inner Kongsfjorden, Svalbard: evidence of recent glacial (surge) activity. University of Tromso, Norway.

Svendsen, H., Beszczynska-Moller, A., Hagen, J.O., Lefauconnier, B., Tverberg, V., Gerland, S., Orbaek, J.B., Bischof, K., Papucci, C., Zajaczkowski, M., Azzolini, R., Bruland, O., Wiencke, C., Winther, J.G., Dallmann, W., 2002. The physical environment of Kongsfjorden-Krossfjorden, an Arctic fjord system in Svalbard. Polar Res. 21, 133–166. https://doi.org/10.1111/j.1751-8369.2002.tb00072.x.

Takahashi, T., Sutherland, S.C., Chipman, D.W., Goddard, J.G., Ho, C., Newberger, T., Sweeney, C., Munro, D.R., 2014. Climatological distributions of pH, pCO(2), total CO2, alkalinity, and CaCO3 saturation in the global surface ocean, and temporal changes at selected locations. Mar. Chem. 164, 95–125. https://doi.org/10.1016/j.marchem.2014.06.004.

Thomas, H., Schiettecatte, L.S., Suykens, K., Kone, Y.J.M., Shadwick, E.H., Prowe, A.E.F., Bozec, Y., de Baar, H.J.W., Borges, A.V., 2009. Enhanced ocean carbon storage from anaerobic alkalinity generation in coastal sediments. Biogeosciences 6, 267–274. https://doi.org/10.5194/bg-6-267-2009.

Torres, M.A., Moosdorf, N., Hartmann, J., Adkins, J.F., West, A.J., 2017. Glacial weathering, sulfide oxidation, and global carbon cycle feedbacks. PNAS 114, 8716–8721. https://doi.org/10.1073/pnas.1702953114.

Turk, D., Bedard, J.M., Burt, W.J., Vagle, S., Thomas, H., Azetsu-Scott, K., McGillis, W.R., Iverson, S.J., Wallace, D.W.R., 2016. Inorganic carbon in a high latitude estuary-fjord system in Canada's eastern Arctic. Estuar. Coast. Shelf Sci. 178, 137–147. https://doi.org/10.1016/j.ecss.2016.06.006.

Tynan, E., Clarke, J.S., Humphreys, M.P., Ribas-Ribas, M., Esposito, M., Rerolle, V.M.C., Schlosser, C., Thorpe, S.E., Tyrrell, T., Achterberg, E.P., 2016. Physical and biogeochemical controls on the variability in surface pH and calcium carbonate saturation states in the Atlantic sectors of the Arctic and Southern Oceans. Deep-Sea Research Part Ii-Topical Studies in Oceanography 127, 7–27. https://doi.org/10.1016/j.dsr2.2016.01.001.

Tyrrell, T., Merico, A., 2004. Emiliania huxleyi: bloom observations and the conditions that induce them. In: Coccolithophores: From Molecular Processes to Global Impact, pp. 75–97.

Uppström, L.R., 1974. The boron/chlorinity ratio of deep-sea water from the Pacific Ocean. Deep-Sea Res. Oceanogr. Abstr. 21, 161–162. https://doi.org/10.1016/0011-7471(74)90074-6.

Vihtakari, M., Welcker, J., Moe, B., Chastel, O., Tartu, S., Hop, H., Bech, C., Descamps, S., Gabrielsen, G.W., 2018. Black-legged kittiwakes as messengers of Atlantification in the Arctic. Sci. Rep. 8 https://doi.org/10.1038/s41598-017-19118-8.

Wolf-Gladrow, D.A., Zeebe, R.E., Klaas, C., Körtzinger, A., Dickson, A.G., 2007. Total alkalinity: The explicit conservative expression and its application to biogeochemical processes. Mar. Chem. 106, 287–300. https://doi.org/10.1016/j.marchem.2007.01.006.